16060DDZ12/69

PB190791

REUTILIZATION OF WASTEWATER RECYCLED THROUGH GROUND WATER

Volume II

Appendices 1, 2, 3

Appendix 1	Well Data, including Chemical and Bacterial Analyses and Ground Water Surface Elevations
Appendix 2	Chemical Quality of Water from Piezometers
Appendix 3	Complete Report of Geophysical Investigation of the Upper San Jacinto Ground Water Basin

Demonstration Project Grant FWPCA 16060 DDZ

December 1968

Reproduced by the
CLEARINGHOUSE
for Federal Scientific & Technical
Information Springfield Va. 22151

Eastern Municipal Water District
Hemet, California

107

REUTILIZATION OF WASTEWATER RECYCLED THROUGH GROUND WATER

PROGRESS REPORT 1965-1968

DEMONSTRATION PROJECT GRANT FWPCA 16060 DDZ

DECEMBER 1968

VOLUME II

Eastern Municipal Water District
24530 San Jacinto Street
Post Office Box 858
Hemet, California 92343

ROSTER OF GOVERNING BODIES

PROJECT CONTROL BOARD

Doyle F. Boen	Eastern Municipal Water District
Richard A. Bueermann	Santa Ana River Basin Regional Water Quality Control Board
Dr. Albert F. Bush	University of California
James E. Lenihan	Eastern Municipal Water District
Dr. Harvey F. Ludwig	Engineering-Science, Inc.
Dr. Jack E. McKee	California Institute of Technology

PROJECT ADVISORY COMMITTEE

Paul R. Bonderson	California Water Resources Control Board
Arthur E. Bruington	Los Angeles County Flood Control District
Robert J. Chun (1966-Present)	California Department of Water Resources
Robert O. Eid	Riverside County Flood Control and Water Conservation District
Maurice B. Hawkins	Riverside County Health Department
John D. Parkhurst	Los Angeles County Sanitation Districts
Arthur W. Reinhardt	California Department of Public Health
David B. Willetts (1965-66)	California Department of Water Resources

BOARD OF DIRECTORS
EASTERN MUNICIPAL WATER DISTRICT

W. M. Kolb	President
Floyd C. Bonge	Vice President
Merlyn L. McIntyre	Member
Albert W. Eggen	Member
J. Langdon Maxwell	Member

PROJECT DIRECTOR

Doyle F. Boen	General Manager and Chief Engineer Eastern Municipal Water District

PROJECT ENGINEER

James E. Lenihan	Sanitary Engineer Eastern Municipal Water District

NOTICE TO USERS

Portions of this document have been judged by the Clearinghouse to be of poor reproduction quality and not fully legible. However, in an effort to make as much information as possible available to the public, the Clearinghouse sells this document with the understanding that if the user is not satisfied, the document may be returned for refund.

If you return this document, please include this notice together with the IBM order card (label) to:

Clearinghouse
Attn: 152.12
Springfield, Va. 22151

TABLE OF CONTENTS

Frontispiece

Table of Contents

APPENDIX 1	Well Data, including Chemical and Bacterial Analyses and Ground Water Surface Elevations
APPENDIX 2	Chemical Quality of Water from Piezometers
APPENDIX 3	Complete Report of Geophysical Investigation of the Upper San Jacinto Ground Water Basin

APPENDIX 1

WELL DATA, INCLUDING CHEMICAL AND BACTERIAL ANALYSES AND GROUND WATER SURFACE ELEVATIONS

The water analyses on the following pages are listed by township, range, section, 40-acre parcel and number of well in 40-acre parcel.

e.g., 4S1W 23N2 means

Township 4 South, Range 1 West

Section 23, 40-acre parcel N

Well No. 2 in the 40-acre parcel

Forty-acre parcels are contained within a 1 square mile section, as shown below:

1 section

D	C	B	A
E	F	G	H
M	L	K	J
N	P	Q	R

The abbreviations on the following pages are as follows:

Ca - Calcium
Mg - Magnesium
Na - Sodium
K - Potassium
F - Fluoride
B - Boron
MBAS - Methylene Blue Alkyl Surfactants

CO_3 - Carbonate
HCO_3 - Bicarbonate
SO_4 - Sulfate
Cl - Chloride
NO_3 - Nitrate
TDS - Total Dissolved Solids
EC - Electrical Conductivity
Total Hardness as Calcium Carbonate

WELL LOCATION MAP

TOWNSHIP 4 SOUTH
RANGE 1 WEST
SCALE 1" = 2000'

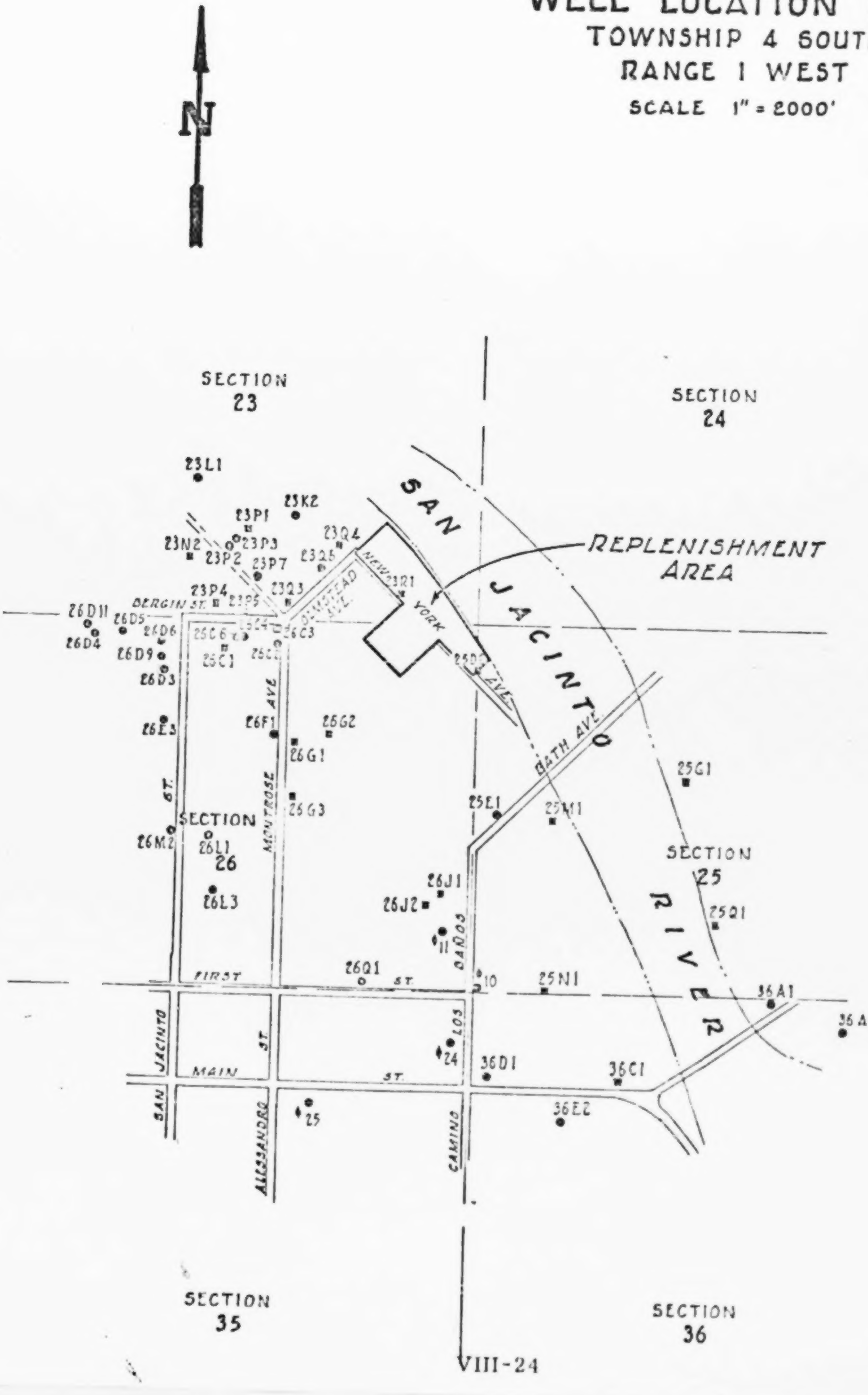
N
SECTION 23
SECTION 24
SECTION 25
SECTION 26
SECTION 35
SECTION 36
SAN JACINTO RIVER
REPLENISHMENT AREA
BERGIN ST.
OLMSTEAD AVE.
NEW YORK AVE.
BATH AVE.
MONTROSE AVE.
SAN JACINTO ST.
ALESSANDRO ST.
CAMINO LOS BAÑOS
FIRST ST.
MAIN ST.
23L1
23K2
23P1
23N2
23P3
23P2
23P7
23Q4
23Q5
23R1
23P4
23P5
23Q3
26D11
26D5
26D6
26D4
26D9
26D3
26C6
26C4
26C3
26C1
26C2
25D3
26E3
26F1
26G2
26G1
26G3
26M2
26L1
26L3
26J1
26J2
11
10
26Q1
25E1
25M1
25G1
25Q1
25N1
36A1
36A2
24
36D1
36C1
36E2
25

WELL DATA

Chemical Analyses
(milligrams per liter)

Well No.	Date	EC x 10^6 @ 25° C	pH	Ca	Mg	Na	K	CO_3	HCO3	SO_4	Cl	NO_3	Total Hardness	F	B	MBAS	TDS
4S1W 23N2	10/65	310	7.7	38	4	22	1	0	174	6	12	0	112	0.3	0.1	0	206
	1/67	415	7.8	50	7	26	3	0	189	20	23	2	152	0.2	0.1	0	257
	11/68	400	7.5	36	10	14	0.2	0	144	8	19	5	129	0.3	0.1	0	244
4S1W 23P1	5/65	332	7.8	42	4	22	4	0	171	25	11	0	124	0.2	-	-	210
	12/66	460	7.7	61	6	29	3	0	165	80	18	1	178	0.4	0.3	0.1	332
4S1W 23P4	10/65	370	7.7	48	6	26	2	0	177	33	16	0	144	0.4	0.1	0	255
	11/68	400	7.6	47	6	11	2	0	150	17	20	2	141	0.5	Tr.	0	263
S1W 23Q3	5/65	290	7.4	42	4	21	2	0	177	2	14	0	124	0.2	0	0	215
	12/66	430	8.0	52	4	34	3	0	183	32	32	0	148	0.3	0.3	0.0	286
	4/67	479	7.5	55	5	35	3	0	173	36	38	0.4	157	0.3	0.4	0	272
4S1W 23Q4	5/65	264	8.7	18	2	36	5	30	85	2	18	0	56	0.5	-	-	168
	12/66	350	7.6	27	5	37	4	0	159	19	25	0	90	0.4	0.3	0.1	226
	4/67	385	7.2	45	9	34	4	0	184	39	28	0.4	148	0.2	0.4	0	296
	11/68	575	7.6	50	17	26	6	0	161	93	22	4	194	0.5	Tr.	Tr.	325
S1W 25G1	9/61	526	7.4	58	4	42	2	0	235	25	28	0	160	-	-	-	-
	3/63	576	8.2	61	9	40	2	6	241	40	27	0	190	0.6	-	-	370
	10/65	540	8.0	64	8	46	2	0	244	33	30	6	192	0.9	0.2	0	370
	10/65	540	7.8	64	5	50	2	0	235	60	23	0	180	0.4	0.1	0	365
	3/68	720	7.8	72	10	53	4	0	232	96	32	1	220	0.4	0.3	0	430
	6/68	720	7.2	69	13	52	5	0	217	105	43	1	228	0.5	0.1	0	461
	11/68	725	7.5	66	18	43	6	0	189	106	46	2	237	0.4	0.2	0	502
S1W 25M1	5/65	385	7.8	48	3	29	3	0	183	19	18	1	134	0.4	-	0	243
	10/65	330	8.0	46	4	28	1	0	195	22	16	3	132	0.7	0	0	255
	5/67	405	7.9	49	6	25	2	0	193	25	15	0.4	147	0.04	0.1	-	179
4S1W 25N1	3/63	379	7.9	54	3	21	2.7	0	177	21	14	1.6	148	0.2	0.02	-	213
	10/65	360	7.7	51	4	26	2	0	177	27	14	7	144	0.2	0.1	0	244
	4/67	376	7.6	50	4	25	2	0	171	26	15	6.2	140	0.5	0.2	-	206
4S1W 26G1	1/61	355	7.7	42	4	24	1	0	177	10	14	0	122	-	-	-	272
	3/63	687	7.6	98	11	31	3.5	0	253	64	34	41	290	0.03	0.02	-	450
	10/65	310	7.7	40	3	25	2	0	165	15	14	0	112	0.3	0.2	0	212
	12/66	340	8.0	42	3	25	3	0	146	20	21	0	116	0.4	0.4	0	221
	11/68	400	7.5	48	6	19	4	0	148	33	20	4	145	0.2	Tr.	0	270

Well Data
Chemical Analyses continued

Well No.	Date	EC x 10^6 @ 25° C	pH	Ca	Mg	Na	K	CO_3	HCO_3	SO_4	Cl	NO_3	Total Hardness	F	B	MBAS	TDS
4S1W 26G2	10/65	330	7.8	42	3	26	2	0	180	13	14	0	116	0.4	0.1	0	215
	5/67	513	7.9	68	9	23	2	0	195	74	20	0.4	207	0.3	0.2	-	266
	11/68	575	7.4	74	8	16	3	0	157	55	37	21	219	0.1	Tr.	0	382
4S1W 26G3	10/65	520	7.6	67	6	30	4	0	201	52	28	2	192	0.2	0.2	0	320
4S1W 36A1	3/63	394	8.2	48	5	22	2	9	171	17	16	0	140	0.04	-	-	243
	10/65	340	7.7	46	6	26	1	0	186	14	18	0	140	0.3	0.1	0	243
	4/67	251	7.4	40	4	21	1	0	162	10	15	0.4	117	0.4	0.1	-	125
	11/68	410	7.4	34	10	21	4	0	146	12	26	0	127	0.2	0	0	272
EFFLUENT 965-68 Average			7.8	75	12	125	19	0	259	131	114	24	208	0.84	0.69	1.37	674

WELL DATA

Ground Water Surface Elevation

Well No. & Date	Static Level	Elevation
4S1W 23N2		
10/15/65	174'	1363
11/ 2/65	170'	1367
11/12/65	170'	1367
11/19/65	167'	1370
2/13/66	167'	1370
3/ 7/67	167'	1370
11/29/67	169'	1368
10/29/68	186'	1357
4S1W 23P1		
5/19/65	146'	1396
9/14/65	150'	1392
11/ 2/65	150'	1392
11/12/65	150'	1392
11/19/65	150'	1392
2/15/66	149'	1393
3/ 7/67	149'	1393
11/29/67	148'	1394
3/21/68	152'	1390
10/29/68	155'	1387
4S1W 23P4		
10/15/65	174'	1369
11/ 2/65	174'	1370
11/12/65	174'	1370
11/19/65	172'	1372
2/16/66	171'	1373
3/ 7/67	173'	1371
11/29/67	171'	1373
10/29/68	185'	1357
4S1W 23Q3		
5/19/65	162'	1385
6/11/65	164'	1383
9/14/65	169'	1378
10/15/65	169'	1378
11/ 1/65	168.5'	1379
11/12/65	168.5'	1379
11/19/65	168.5'	1379
2/15/66	168.5'	1379
3/ 7/67	168.5'	1379

Well No. & Date	Static Level	Elevation
4S1W 23Q3 continued		
5/17/67	172'	1375
11/29/67	121'	1376
11/ 1/68	181'	1366
4S1W 23Q4		
5/19/65	152.5'	1391
6/11/65	153.5'	1390
9/14/65	155'	1388
10/15/65	156'	1387
11/ 1/65	156.5'	1387
11/12/65	156.5'	1387
11/19/65	155'	1388
2/15/66	156'	1389
3/ 7/67	156.5'	1387
5/17/67	156.5'	1387
11/29/67	157.5'	1386
11/ 1/68	180.5'	1363
4S1W 23R1		
2/15/66	181'	1369
3/ 7/67	190'	1360
5/17/67	189.5'	1360
11/29/67	195'	1355
11/ 1/68	198.5'	1351
11/25/68	199.5'	1350
4S1W 25G1		
11/19/65	196'	1377
4/19/68	189'	1384
11/ 1/68	193.5'	1379
4S1W 25M1		
5/20/65	200'	1373
6/11/65	198'	1375
10/ 4/65	209.5'	1363
10/15/65	209.5'	1363
11/ 2/65	209'	1363
11/12/65	209'	1363
11/19/65	208'	1364
2/15/66	208'	1364
3/ 7/67	209'	1363

Well Data
Ground Water Surface Elevation continued

Well No. & Date	Static Level	Elevation
4S1W 25M1 continued		
5/17/67	156.5'	1387
11/29/67	157.5'	1386
11/ 1/68	180.5'	1363
4S1W 23R1		
2/15/66	181'	1369
3/ 7/67	190'	1360
5/17/67	189.5'	1360
11/29/67	195'	1355
11/ 1/68	198.5'	1351
11/25/68	199.5'	1350
4S1W 25G1		
11/19/65	196'	1377
4/19/68	189'	1384
11/ 1/68	193.5'	1379
4S1W 25M1		
5/20/65	200'	1373
6/11/65	198'	1375
10/ 4/65	209.5'	1363
10/15/65	209.5'	1363
11/ 2/65	209'	1363
11/12/65	209'	1363
11/19/65	208'	1364
2/15/66	208'	1364
3/ 7/67	209'	1363
5/17/67	208'	1364
11/29/67	216.5'	1356
10/28/68	222'	1351
4S1W 25N1		
11/ 4/68	241'	1342
4S1W 26G2		
5/19/65	182'	1372
6/11/65	176'	1380
9/14/65	180'	1376
11/19/65	181.5'	1374
3/ 7/67	183'	1373
11/11/67	183'	1373
10/31/68	194.3'	1362

Well No. & Date	Static Level	Elevation
4S1W 26G3		
10/15/65	64'	1492
11/ 1/65	64'	1492
11/19/65	65'	1491
11/13/68	173'	1382
4S1W 26J1		
5/20/65	196'	1377
6/11/65	196'	1377
7/ 8/65	197'	1376
9/14/65	199'	1374
10/15/65	199.5'	1373
11/ 1/65	199.5'	1373
11/12/65	199.5'	1373
11/19/65	199'	1374
2/15/66	195'	1378
3/ 7/67	203'	1370
5/17/67	204.5'	1369
11/29/67	204'	1369
10/28/68	218'	1355
4S1W 26J2		
10/15/65	196.5'	1374
11/ 1/65	196.5'	1374
11/12/65	196.5'	1374
11/19/65	196'	1375
2/15/66	197'	1374
3/ 7/67	201'	1370
5/13/67	201'	1370
11/29/67	204'	1367
10/29/68	208'	1363

APPENDIX 2

CHEMICAL QUALITY OF WATER FROM PIEZOMETERS

APPENDIX 2

Chemical Quality of Water From Piezometers
(milligrams per liter)

Piezometer:	B-3		C-2		C-3			C-C-3		D-3a			D-4	
Date:	11/66	3/69	12/66	2/67	12/66	2/67	5/67	5/67	2/69	12/66	2/67	2/69	11/66	2/69
Analysis														
Calcium	73	-	520	519	84	79	76	112	-	84	95	-	80	-
Magnesium	6	-	91	93	22	21	20	25	-	22	24	-	23	-
Sodium	141	-	94	124	120	116	124	161	-	132	140	-	139	-
Potassium	14	-	10	8	6	3	4	20	-	4	2	-	5	
Ammonia	-	7.8	2	1.4	0.1	0.1	0.1	0.1	1.74	0.6	0.5	0.71	-	0.99
Carbonate	46	-	0	0	0	5	0	0	-	0	10	-	4	-
Bi-Carbonate	46	-	207	143	244	198	220	262	-	287	315	-	242	-
Sulfate	200	-	1500	1535	150	144	140	276	-	150	167	-	220	-
Chloride	120	-	135	152	131	132	133	138	-	117	117	-	108	-
Nitrate	41	5	6	8	48	44	40	56	0	47	44	2	24	trace
Fluoride	0.5	-	0.2	0.3	1.3	1.0	0.8	0.9	-	0.8	0.7	-	0.8	-
Total Hardness as $CaCO_3$	208	173	1680	1676	300	280	276	382	216	300	337	212	294	196
T. D. S.	707	533	2779	2596	765	706	700	977	3378*	728	773	3757*	726	2631*
Boron	0.47	-	0.4	0.06	0.6	0.55	0.6	0.60	-	0.8	0.56	-	0.27	-
MBAS	-	trace	0.3		0.2	-	0.3	0.3	0	0.2	-	0	-	0
C. O. D. Total	-	34.9	-		-	-	-	-	82.7	-	-	39.4	-	55.2
C. O. D. Dissolved	-	34.9	-		-	-	-	-	39.4	-	-	35.4	-	39.4
Total Nitrogen	-	81.3	-		-	-	-	-	3.74	-	-	1.38	-	1.40
pH	8.8	-	7.1	7.9	7.0	8.0	7.6	7.9	-	7.7	8.1	-	8.2	-
EC x 10^6	1126	-	3600	7975	1120	1169	1100	1511	-	1100	1283	-	1207	-

Appendix 2 continued:

Piezometer:	D-4		D-5	D-D-3		E-3				E-4		E-5	
Date:	5/67	2/69	2/67	5/67	2/69	11/66	12/66	2/67	2/69	11/66	2/69	12/66	2/69
Analysis													
Calcium	82	-	78	93	-	116	96	106	-	79	-	85	-
Magnesium	21	-	20	24	-	19	22	17	-	18	-	19	-
Sodium	120	-	115	131	-	136	128	138	-	133	-	116	-
Potassium	19	-	10	14	-	6	4	3	-	16	-	5	-
Ammonia	0.9	11.9	0.3	0.8	1.25	0.3	0.3	0.3	1.4	-	1.46	0	3.04
Carbonate	0	-	2	14	-	0	0	0	-	0	-	7	-
Bi-Carbonate	259	-	166	298	-	378	287	342	-	224	-	274	-
Sulfate	163	-	146	137	-	150	160	160	-	123	-	137	-
Chloride	126	-	138	144	-	138	121	120	-	124	-	113	-
Nitrate	35	2	51	35	trace	44	48	35	6	78	0	23	trace
Fluoride	0.6	-	0.6	0.8	-	0.7	0.9	0.7	-	0.4	-	0.6	-
Total Hardness as $CaCO_3$	292	216	278	332	306	370	330	338	376	271	184	290	247
T.D.S.	681	1887*	738	731	1936*	851	843	780	1391*	736	1893*	677	2004*
Boron	0.52	-	0.54	0.50	-	0.6	0.8	0.8	-	0.7	-	0.6	-
MBAS	0.22	0	-	0.18	0	0.2	0.3	-	trace	-	trace	-	0
C.O.D. Total	-	30.8	-	-	71.0	-	-	-	61.8	-	22.2	-	26.5
C.O.D. Dissolved	-	22.1	-	-	53.3	-	-	-	39.7	-	22.2	-	22.1
Total Nitrogen	-	12.28	-	-	1.49	-	-	-	1.57	-	1.38	-	3.19
pH	7.6	-	8.2	8.1	-	7.8	8.0	8.2	-	8.1	-	8.2	-
EC x 10^6	1173	-	1203	1274	-	1260	1240	1333	-	1166	-	1165	-

Appendix 2 continued:

Piezometer: Date:	A-2 3/69	B-2 3/69	BB-1 3/69	C-1 3/69	C2-2 3/69	D1-1 3/69	D-2 2/69	E-1 3/69	E3-3 2/69	F-3 2/69	F-4 2/69	G-3 2/69	G-5 2/69	Effluent Average 1965-68
Analysis														
Calcium	-	-	-	-	-	-	-	-	-	-	-	-	-	75
Magnesium	-	-	-	-	-	-	-	-	-	-	-	-	-	12
Sodium	-	-	-	-	-	-	-	-	-	-	-	-	-	125
Potassium	-	-	-	-	-	-	-	-	-	-	-	-	-	19
Ammonia	trace	1.11	7.37	1.65	trace	trace	0.90	trace	trace	2.79	4.25	0.86	trace	15
Carbonate	-	-	-	-	-	-	-	-	-	-	-	-	-	0
Bi-Carbonate	-	-	-	-	-	-	-	-	-	-	-	-	-	259
Sulfate	-	-	-	-	-	-	-	-	-	-	-	-	-	131
Chloride	-	-	-	-	-	-	-	-	-	-	-	-	-	114
Nitrate	0	0	trace	2	0	14	trace	51	2	27	4	50	9	24
Fluoride	-	-	-	-	-	-	-	-	-	-	-	-	-	0.84
Total Hardness as $CaCO_3$	364	754	600	542	370	232	243	361			247	302		208
T.D.S.	858	1633	1145	1128	960	653	3443*	818			2122*	2059*		674
Boron	-	-	-	-	-	-	-	-	-	-	-	-	-	0.69
MBAS	0	trace	0	trace	0	0	0	0	-	-	trace	0	-	1.37
C.O.D. Total	26.2	26.4	43.8	105	61.1	35.0	82.7	26.2	44.2	75.0	35.3	17.6	348	-
C.O.D. Dissolved	17.5	17.6	17.6	21.9	30.6	30.6	39.4	21.9	26.5	70.5	30.8	8.8	61.8	-
Total Nitrogen	0.20	1.90	11.17	2.32	0.42	0.49	1.53	0.30	-	-	5.7	4.12		-
ph	-	-	-	-	-	-	-		-	-	-	-		7.4
EC x 10^6	-	-	-	-	-	-	-		-	-	-	-		1130

*Sulfuric Acid added to samples as preservative increased T.D.S.

APPENDIX 3

COMPLETE REPORT OF GEOPHYSICAL INVESTIGATION OF THE UPPER SAN JACINTO GROUND WATER BASIN

GEOPHYSICAL INVESTIGATION OF THE SAN JACINTO VALLEY, RIVERSIDE COUNTY, CALIFORNIA

for

EASTERN MUNICIPAL WATER DISTRICT
HEMET, CALIFORNIA

by

JOHN D. FETT AND ASSOCIATES
26745 MERIDIAN STREET
HEMET, CALIFORNIA
DECEMBER 1967

ABSTRACT

The subsurface geology was investigated in the San Jacinto valley of Riverside County, California by geophysical methods to understand better a segment of the San Jacinto fault zone and the bedrock configuration. Bedrock is sufficiently shallow beneath the southwest portion of the valley to be the major factor controlling ground water conditions.

A gravity survey was successful in determining the bedrock topography beneath the southwest side of the valley where bedrock depth is generally less than 1,000 feet. The drainage patterns on the buried bedrock surface are plotted for the southwest side of the valley.

Because of great depth to bedrock on the northeast side of the valley and lack of knowledge of the bulk density of the deeper sedimentary rock, the gravity survey yielded only qualitative findings on this side of the valley. A seismic refraction survey was then conducted to determine quantitatively the bedrock depth on the northeast side of the valley. Beneath this side of the valley, faulting has dropped bedrock to a depth of about 8,000 feet. This rift is bounded on the southwest by the Casa Loma fault, which passes through the center of the valley, and on the northeast by the Claremont fault, which forms the northeast edge of the valley.

TABLE OF CONTENTS

Introduction 1

Geology 3

Gravity Survey 12

Seismic Survey 18

Findings and their Implications 39

Acknowledgements 52

References 53

Appendix: Gravity Data 56

Appendix: Seismic Data 64

Appendix: Annotated Bibliography, San Jacinto Basin 75

LIST OF FIGURES

Figure		Page
1	Location and Regional Geology	2
2	Generalized Geologic Map	4
3	Bedrock Elevations from Well Log Data	6
4	Location of Gravity Stations	13
5	Bouguer Gravity Anomaly Map	14
6	Bouguer Anomaly Map with Regional Gravity Removed	16
7	Locations of Sections, Seismic Lines and Shot Points	19
8	Travel-Time Graph for Line A	22
9	Seismic Record CIT-V, Line A, Shot Point 1	24
10	Seismic Record 8, Line A, Shot Point 2	26
11	Travel-Time Graph for Line B	28
12	Seismic Record 6, Line B, Shot Point 2	31
13	Travel-Time Graph for Line C	32
14	Travel-Time Graph for Line D	36
15	Drainage Patterns on the Buried Bedrock Surface	40
16	Geologic Section A	43
17	Geologic Section B	45
18	Geologic Sections C and D	46
19	Geologic Section E	48
20	Block Diagram of the San Jacinto Valley	51

INTRODUCTION

The San Jacinto fault is one of the most active faults in Southern California. This report presents a gravity and seismic survey conducted along a portion of the San Jacinto fault zone near the cities of San Jacinto and Hemet, Riverside County, California.

A brief discussion of the geology of the area of investigation will be presented to assist in understanding the subsurface information obtained from the geophysical work.

The gravity survey was effective in outlining the buried bedrock topography on the Hemet side of the San Jacinto Valley where depth to bedrock is generally less than 1,000 feet. On the San Jacinto side of the valley, depth to bedrock was found to be in excess of 3,500 to 4,000 feet and difficult to accurately determine gravimetrically. The gravity work did indicate the location of the deepest portion of the valley and this location was the first to be seismically investigated. The finding was a one and one half mile depth to bedrock in the three mile wide graben formed by the Casa Loma and Claremont branches of the San Jacinto fault zone.

Illuminated by the geophysical findings, the ground water geology and engineering geology of the valley will be discussed in the last section of the report.

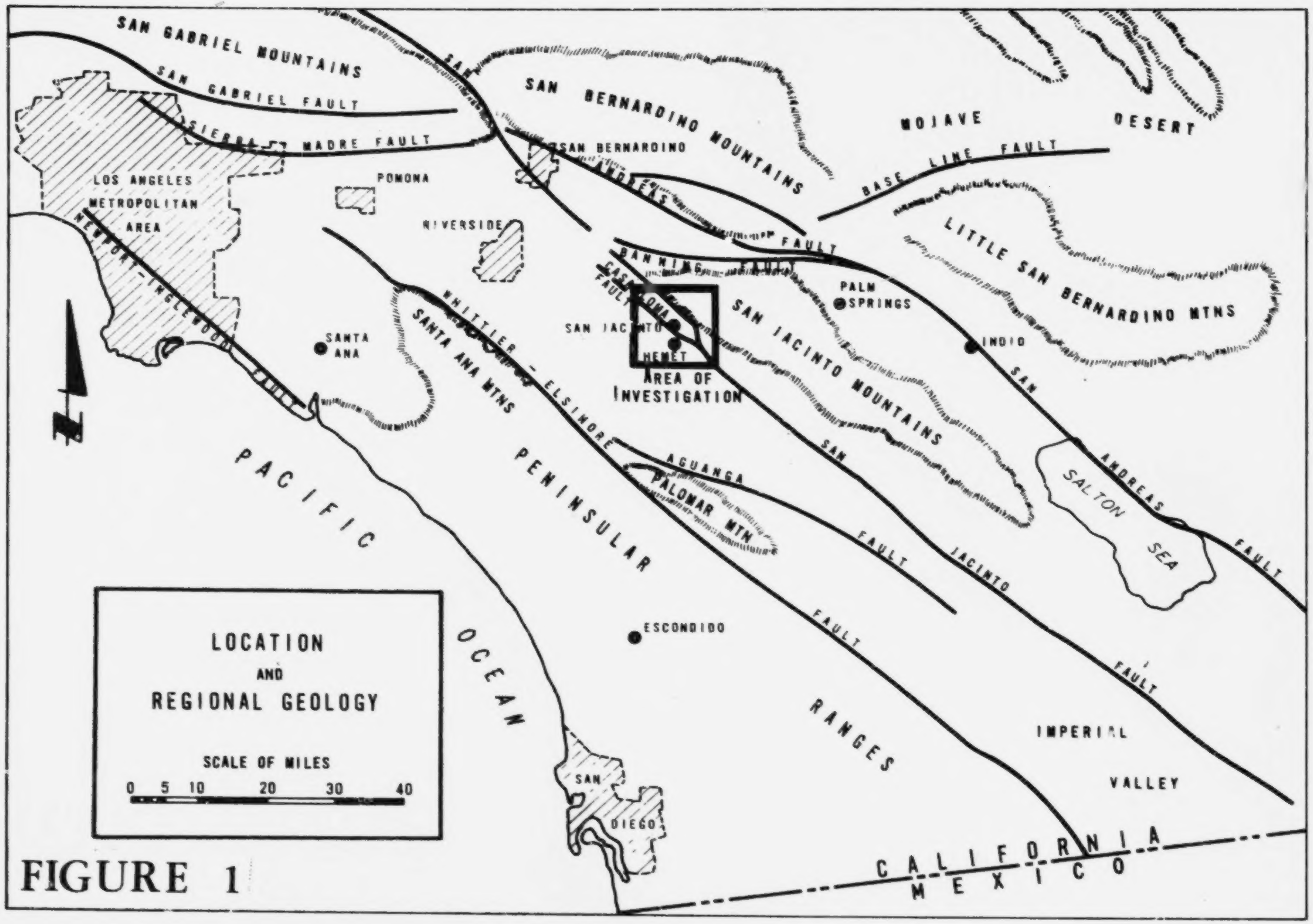

FIGURE 1

LOCATION
AND
REGIONAL GEOLOGY

SCALE OF MILES
0 5 10 20 30 40
SAN GABRIEL MOUNTAINS
SAN GABRIEL FAULT
SIERRA MADRE FAULT
LOS ANGELES METROPOLITAN AREA
NEWPORT-INGLEWOOD FAULT
POMONA
RIVERSIDE
SAN BERNARDINO
SAN BERNARDINO MOUNTAINS
SAN ANDREAS FAULT
MOJAVE DESERT
BASE LINE FAULT
LITTLE SAN BERNARDINO MTNS
BANNING FAULT
CASA LOMA FAULT
SAN JACINTO
HEMET
AREA OF INVESTIGATION
PALM SPRINGS
INDIO
SAN JACINTO MOUNTAINS
SAN JACINTO FAULT
SALTON SEA
SANTA ANA
WHITTIER - ELSINORE FAULT
SANTA ANA MTNS
AGUANGA FAULT
PALOMAR MTN
PENINSULAR RANGES
ESCONDIDO
IMPERIAL VALLEY
PACIFIC OCEAN
SAN DIEGO
CALIFORNIA
MEXICO
N

GEOLOGY

REGIONAL GEOLOGY

Figure 1 indicates the regional geology and the location of the area of investigation.

The area of investigation is at the northern end of the Peninsular Range. Obliquely traversing the Peninsular Range are several parallel fault zones trending northwest-southeast. The San Jacinto fault zone passes through the area of investigation. The San Andreas fault zone is to the northeast and the Elsinore (Whittier-Elsinore) fault zone is to the southwest. On the basis of seismicity in historical time, the San Jacinto fault zone is perhaps the most active in southern California (Allen et al., 1966). Between the San Jacinto and Elsinore fault zones is the Perris Block, a relatively stable geomorphic unit named by English (1926) and its geomorphology discribed by Dudley (1936). The Hemet side of the San Jacinto valley is on the edge of the Perris Block and the San Jacinto side of the valley is on the San Jacinto fault zone.

A rift or graben, bounded by the Casa Loma and Claremont branches of the San Jacinto fault system (figure 2), exists beneath San Jacinto.

A similar structure exists in the Elsinore fault zone. A lava flow, probably of late Pliocene or early Pleistocene age, has been dropped at least 3,000 feet by faulting and covered by more than 2,400 feet of graben filling sediments,

FIGURE 2

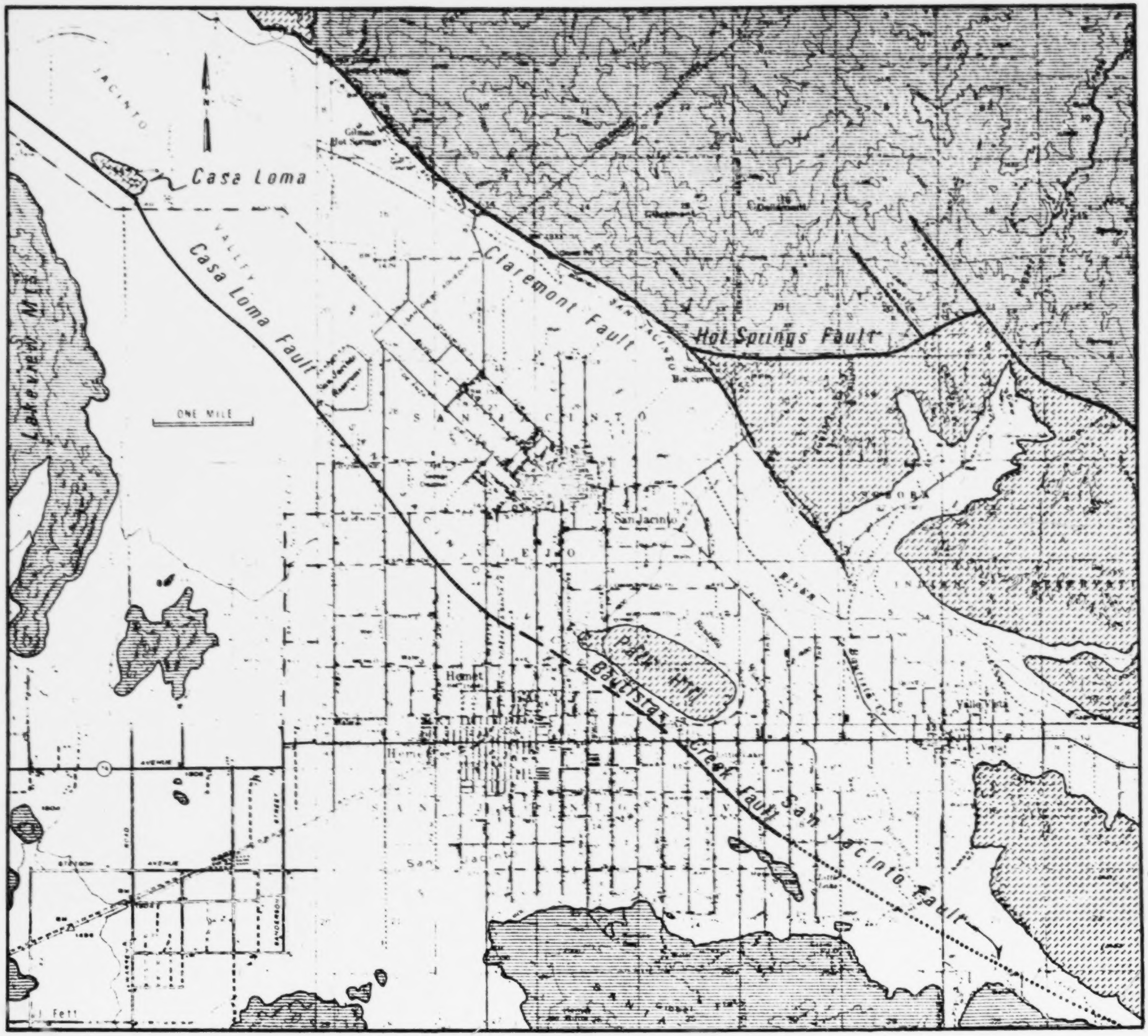
Casa Loma
JACINTO
VALLEY
Casa Loma Fault
Claremont Fault
Hot Springs Fault
SAN JACINTO
San Jacinto
RIVER
Park Hill
Bautista Creek Fault
San Jacinto Fault
Hemet
Valle Vista
Lakeview Mts
ONE MILE

Geologic Units

LATE QUATERNARY

☐ Alluvium, Alluvial Soil, & Terrace Deposits

EARLY QUATERNARY

– LATE TERTIARY

▨ Non-Marine Sedimentary Rocks

PRE-TERTIARY

▨ Crystalline Igneous & Metamorphic Rocks

ONE MILE

Generalized Geologic Map of the San Jacinto Valley Area

(Mann, 1955).

LOCAL GEOLOGY

The geologic relations in the area are largely controlled by faulting. Alluvium has been deposited against faulted blocks. To the southwest of the Casa Loma fault, alluvium has been deposited against remnant high points of metamorphic and igneous rocks. The alluvium itself has been cut by faults, some forming escarpments at the surface. Other faults are indicated by anomalous ground water conditions. Figure 2 is a map of the local geology generalized by the writer from the state geologic map (Rogers, 1965). Figure 3 presents bedrock elevations determined from well logs. The well data northwest of Hemet are from Bean (1955); the remainder have been gathered by the writer. No wells have reached bedrock between the Casa Loma and Claremont faults in the area of investigation.

Geologic Formations

The metamorphic rocks are mostly schists and gneisses. They have been assigned to the Paleozoic Era by Larsen (1948).

The igneous rocks are mostly Cretaceous tonalites and granodiorites. These plutonics are part of the southern California batholith and are described by Larsen (1948).

Since the densities and especially the seismic velocities of the metamorphic and igneous rocks are similar, these rocks are not differentiated on the generalized geo-

FIGURE 3

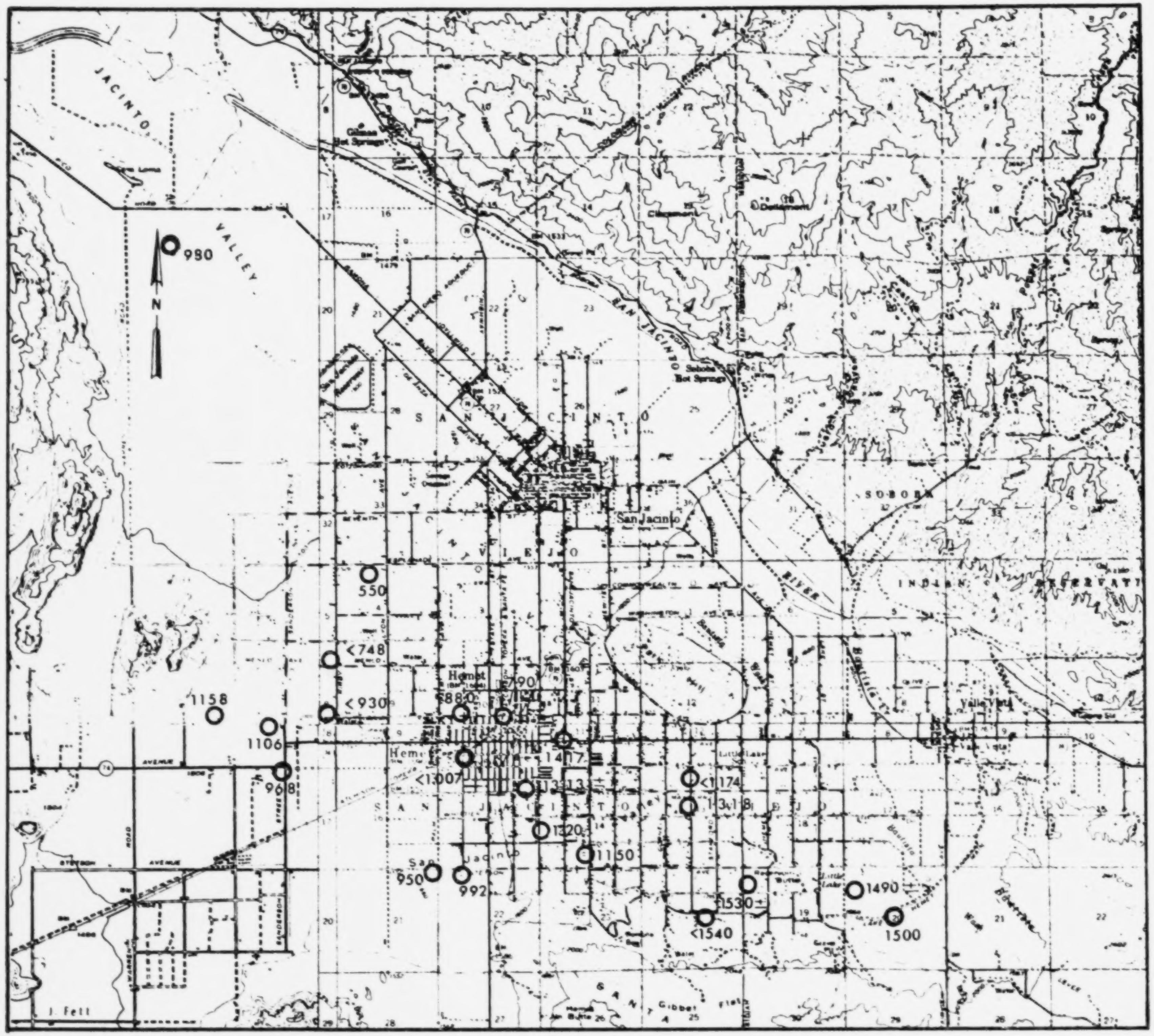
JACINTO
VALLEY
N
980
1158
1106
968
550
<748
<930
880
790
<1007
1417
1313
1320
1150
950
992
<1174
1318
1530±
<1540
1490
1500
San Jacinto
Hemet
SAN JACINTO
SOBOBA
INDIAN RESERVATION
RIVER
Valle Vista
Little Lake
Soboba Hot Springs
AVENUE

NOT REPRODUCIBLE

Bedrock Elevations

From Well Log Data

ONE MILE

ELEVATIONS IN
FEET ABOVE SEA LEVEL

logic map. Both may be considered as impermeable, nonwater-bearing rocks, though for small water supplies the greater fracturing and depth of weathering in the metamorphics tend to make them more productive than the igneous rock.

The early Quaternary - late Tertiary sediments of the area were named by Frick (1921) and divided by him into the Mt. Eden, San Timoteo, and Bautista Formations. Based on vertebrate faunas he assigned them to the Upper Lower Pliocene, late Pliocene and Pleistocene, respectively. They are all poorly consolidated continental clastics, generally of rather low permeability. These older sediments form Park Hill, Casa Loma, the hills east of Bautista wash, the Badlands to the northwest of the area of investigation, much of the Soboba reservation, and the sediments of the southwest side of the San Jacinto mountains.

The Recent - late Pleistocene sediments fill much of the San Jacinto valley and most are stream channel deposits. Some thin silt and clay layers were deposited by flooding and contemporaneous weathering increased the content of the residual clay.

Faults

The Casa Loma fault forms the northeast boundary of the Perris Block in the area of investigation. A Recent scarp exists along this fault, extending from Casa Loma to Park Hill. It has a maximum height of over 20 feet, the northeast side having dropped relative to the southwest side.

Trenches across this fault were dug for the Los Angeles and San Diego branches of the Colorado River aqueduct and these excellent exposures of the fault's Recent activity were described by Buwalda (Bean, 1955) and by Proctor (1962). The fault hampers the flow of ground water; differences of as much as 50 feet in the water table have occured across the fault immediately west of Park Hill.

To the south and southeast of Park Hill, Bean located a fault by geomorphic and hydrologic evidence. He named it the Bautista Creek fault. It has a scarp of a few feet to six feet in height, the northeast side having dropped relative to the southwest side. This fault has moved in the same sense as the Casa Loma and is well aligned with it. The writer suggests they are essentially the same fault. The segment of Recent scarp southwest of Park Hill has been removed by erosion. Down-faulting of the area to the northeast of the fault formed a closed topographic depression between the fault scarp and Park Hill. Subsequent flooding and overflow caused the above mentioned erosion of the scarp segment. Bean noted that the Bautista Creek fault meets the Casa Loma fault west of Park Hill but felt there are many dissimilarities between them. He cited the absence of a low scarp along the Bautista Creek fault in the alluvium and the lack of irregularity of trace in its exposures southeast of the valley. Hence he believed the Bautista Creek fault to have marked strike-slip movement as opposed to dip-slip movement on the

Casa Loma fault. On the first point, Bean evidently did not notice the low scarp that does exist along a mile and a half of the Bautista Creek fault. If the Bautista Creek fault were to have a large dip-slip component in the San Jacinto valley, depth to basement would be much greater to the northeast of the fault and the gravity and seismic work investigated this question.

Bean continued the Bautista Creek fault to the southeast of the valley and when the faults southeast of the valley were later studied by Sharp (1967), Sharp called this same fault the San Jacinto fault.

On the north side of the San Jacinto valley the Claremont branch of the San Jacinto fault zone is located at the contact between the valley fill and the steep metamorphic and igneous mountains to the north (Fraser, 1931 and Bean, 1955). The mountains to the north have been elevated along this fault to 3,000 feet above the valley floor. Minimal erosion on the mountain face and extremely small alluvial fans at its foot indicate the recentness of this movement.

Near the center of the valley, Bean located the Park Hill fault along the north side of Park Hill and continued it to the southeast. He noted that it does not appear to have an effect on ground water in the recent sediments. The writer has seen no positive evidence of this fault and has omitted it from the generalized geologic map.

Landslides

Numerous landslides have occurred in the Bautista sediments. Recent occurrences are mostly the result of embankment steepening by river erosion or faulting. Undoubtedly, movement of many of these slides has been triggered by earthquakes. Townley (1918) reported the occurrence of slides during the 1918 earthquake.

Subsidence

Three forms of subsidence are occurring in the San Jacinto valley.

Tectonic lowering of the graben bounded by the Casa Loma and Claremont branches of the San Jacinto fault zone has created a closed topographic depression north of the Lakeview mountains. Historically, the depression has been filled with flood water to form a dry lake (Waring, 1919).

Subsidence of approximately the same area has been taking place during the past thirty or so years as a result of ground water withdrawal (Fett et al., 1967). The rate of subsidence is currently about 0.1 foot per year. Pipelines, roads, and structures at the edge of the graben are being damaged. Numerous water wells in the graben have failed by axial compression and many more will be destroyed (Fett and Hamilton, 1968). The size and depth of the natural topographic depression north of the Lakeview mountains is increasing due to this new subsidence.

On the Hemet side of the valley, soil collapse occurs beneath a portion of the city of Hemet. Soil possesses the potential hazard of collapse when it has been deposited so loose as to have sufficient void space to hold enough water for the soil's liquid limit to be reached (Gibbs and Bara, 1967). Wind-deposited silt is the probable local origin of these dangerous soils. No matter how small the foundation loading, if a structure's foundation does not extend below these soils, the structure will settle if the soil becomes saturated. This has occurred to several buildings in the city of Hemet and will probably damage more in the future. It is quite possible that these soils exist at other locations in the San Jacinto valley but have gone unnoticed because of sparse building development in the past.

GRAVITY SURVEY

The gravity survey used LaCoste and Romberg G-22 geodetic gravity meter. It is a portable, temperature-regulated meter working on the zero-length spring principle. It is characterized by small drift without tares.

The locations of most gravity stations of this survey are indicated on figure 4. Some additional stations were occupied outside the area of investigation to obtain insight into the regional gravity anomaly. Station locations, elevations, observed gravity, and anomalies are presented in tabular form in the appendix.

The gravity work presented here is only the writer's portion of a larger project conducted by Dr. Gordon P. Eaton and the writer. The gravity data of the larger project are being reduced in detail by electronic computer. The gravity anomalies plotted here have been reduced by desk calculator. The resulting Bouguer anomaly is presented in figure 5.

A small error has been introduced by ignoring the terrain correction. Most stations are on the rather flat valley floor. At these stations, the error introduced by ignoring the terrain correction for nearby topographic irregularities is negligible. At these stations, a larger error is introduced by ignoring the terrain correction for distant topography, such as the mountains north and east of the valley. This larger error is smoothly varying across

FIGURE 4

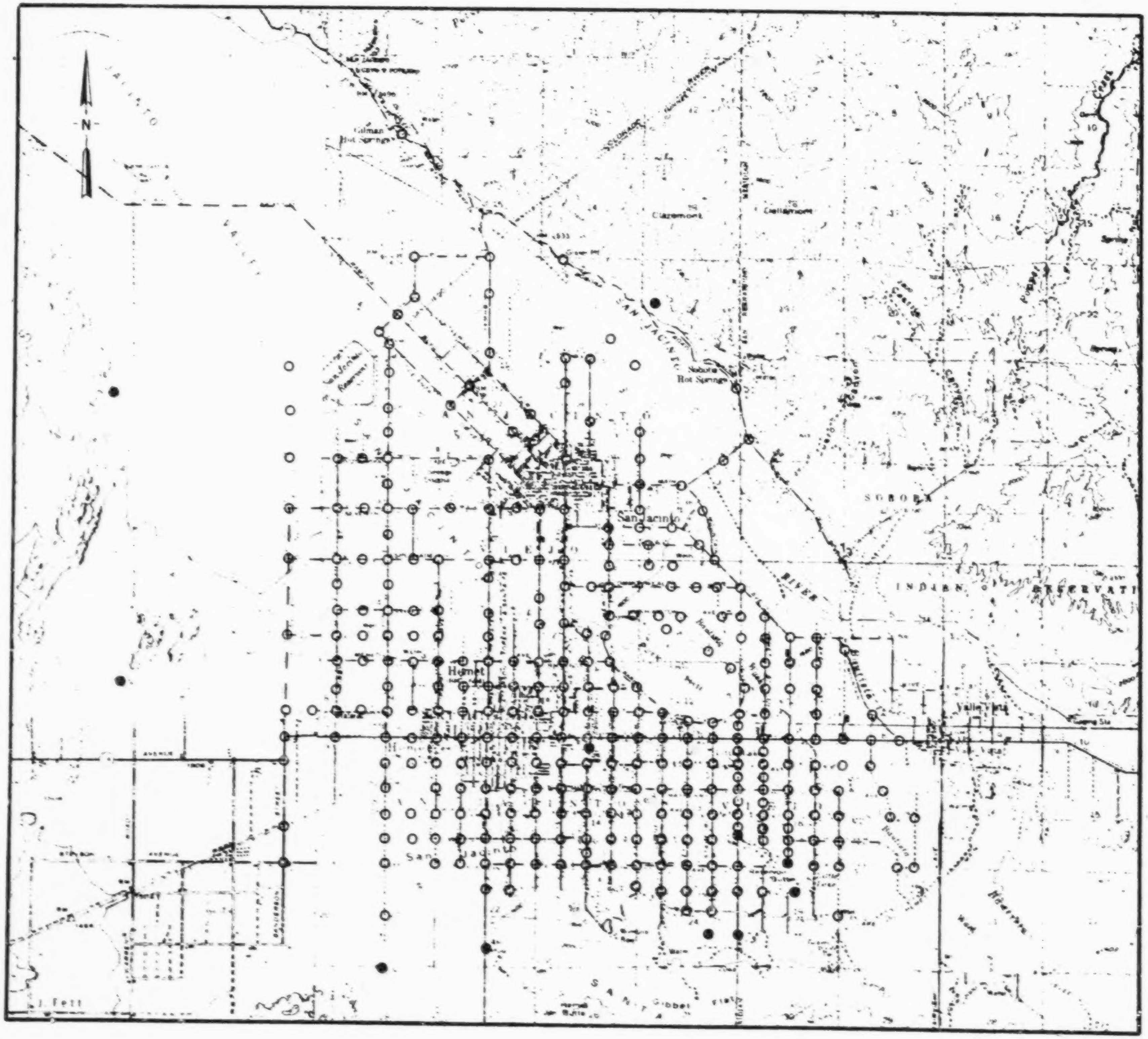
N
SAN JACINTO
VALLEY
Gilman Hot Springs
Soboba Hot Springs
SAN JACINTO
RIVER
SOBOBA
INDIAN RESERVATION
San Jacinto
Hemet
Valle Vista
San Jacinto
SAN JACINTO
Gibbet Flats
Hemet Butte
J. Fett

NOT REPRODUCIBLE

Location of

Gravity Stations

ONE MILE

● Gravity Station On Bedrock

○ Gravity Station On Sediments

FIGURE 5

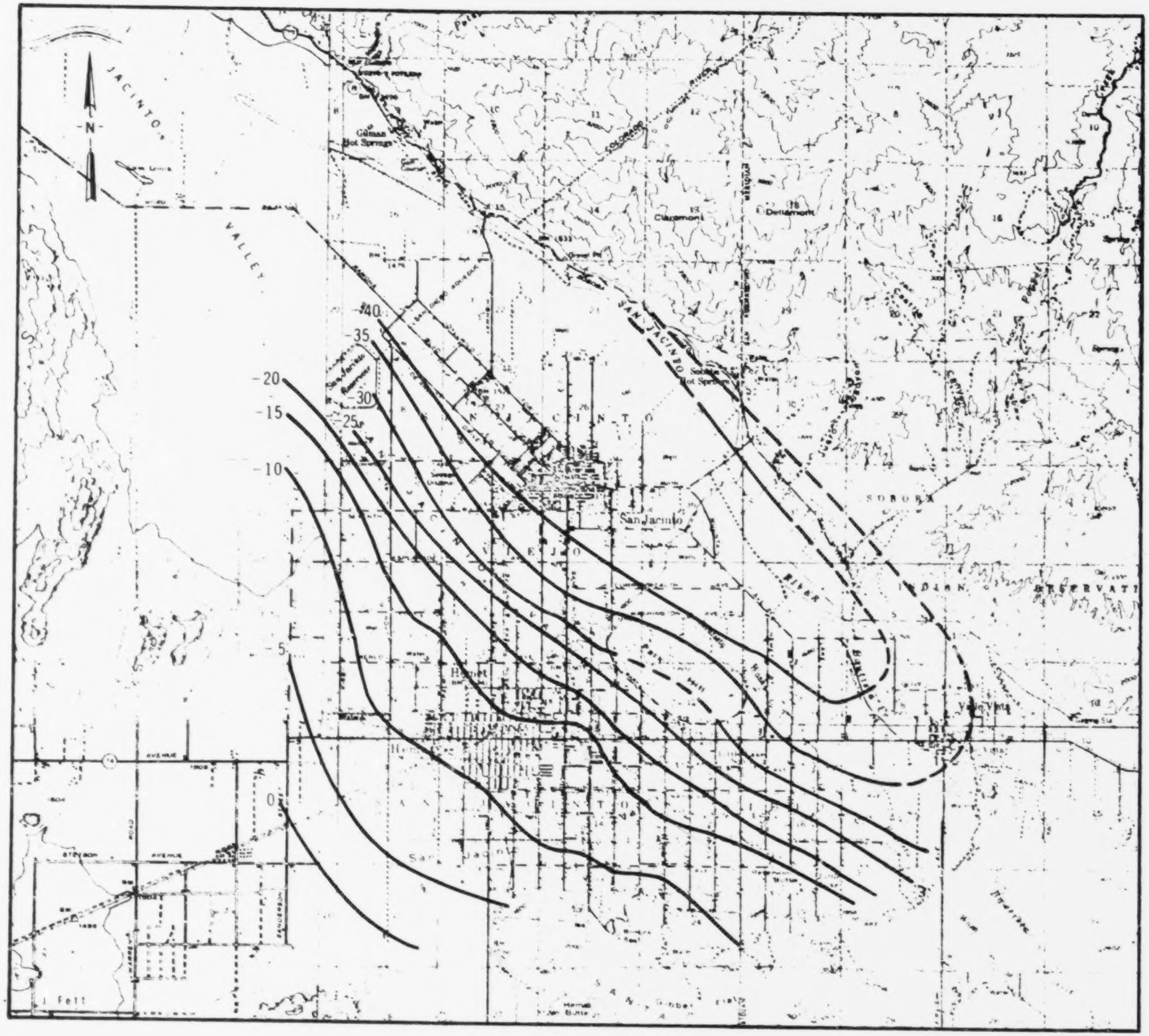
-N-
JACINTO
VALLEY
SAN JACINTO
San Jacinto
SOBOBA
INDIAN RESERVATI
RIVER
Gilman Hot Springs
Claremont
Bautista Cr.
-40
-35
-30
-25
-20
-15
-10
-5
0
J. Fett

NOT REPRODUCIBLE

Bouguer Gravity Anomaly Map

ONE MILE

5 Milligal Contour Interval

Arbitrary Datum

the valley and most of this error will be removed with the regional anomaly.

The error introduced by ignoring the terrain correction for Park Hill was checked for the station nearest the hill and found to be less than 0.3 milligal.

In the area of investigation, the primary causes of the Bouguer anomaly are variation in the thickness of the valley filling sediments and variations in the thickness of the earth's crust. Since the crust is about thirty miles thick beneath the area of investigation, the regional anomaly produced by variation in the crust's thickness is very smooth compared to the anomaly produced by variation in the thickness of the valley sediments.

The anomaly caused by the valley sediments is of interest for this investigation. To extract this local anomaly, the regional anomaly must be removed from the total Bouguer anomaly. In this study, the regional anomaly has been approximated by a linear decrease in gravity, going from the southwest edge of the valley to the northeast edge. The magnitude of this decrease has been adjusted to yield a local anomaly that is approximately zero in value on bedrock on both sides of the valley. The resulting anomaly, figure 6, is due primarily to valley sediments. To the southwest of the Casa Loma fault, this anomaly is approximately proportional to sediment thickness.

To the northeast of the Casa Loma fault, the gravity

FIGURE 6

NOT REPRODUCIBLE

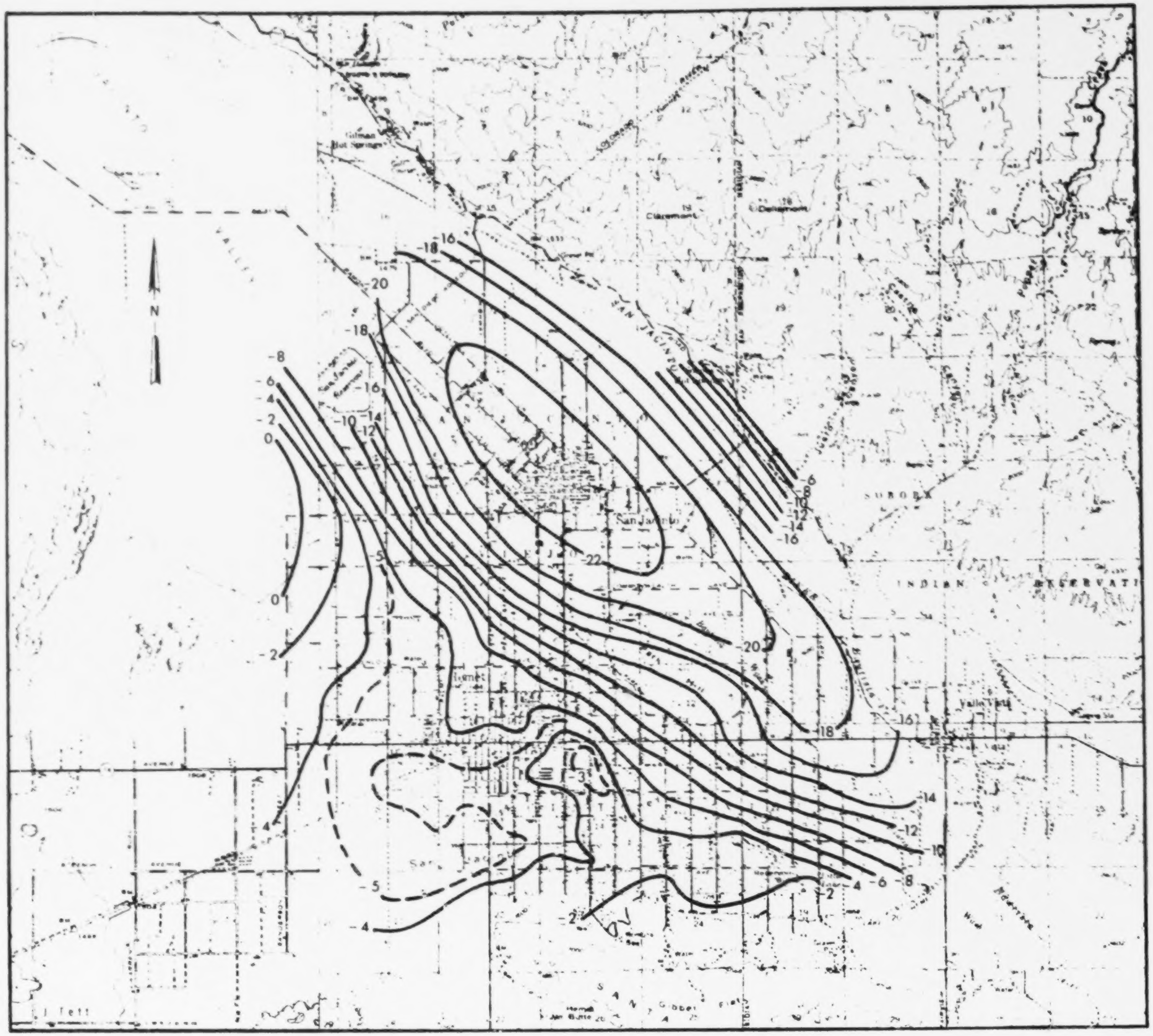
N
SAN JACINTO
San Jacinto
Hemet
Claremont
Gilman Hot Springs
Valle Vista
SOBOBA
INDIAN RESERVATI
VALLEY
-22
-20
-18
-16
-14
-12
-10
-8
-6
-4
-2
0
-3
-5

Bouguer Gravity Anomaly With Regional Removed

ONE MILE

2 Milligal Contour Interval

Arbitrary Datum

anomaly indicates the deepest part of the valley to be approximately beneath the city of San Jacinto. At this location, the anomaly indicates sediment thickness of about 3,500 feet, if a density contrast of 0.5 is assumed.

With sediment depths of 3,000 feet or more, the gravity method of determining depth to bedrock becomes more qualitative than quantitative unless sediment bulk densities are known in detail. The local anomaly is caused by contrast between sediment and bedrock bulk densities. Sediment bulk density increases with greater depth of burial, approaching the density of bedrock. Also, some sediments in the San Jacinto valley have, in the geologic past, been buried to a depth greater than their present depth. Only sparse information is available on sediment bulk densities in the San Jacinto valley and none for depths greater than 1,000 feet.

The greater bulk density of the Bautista Formation sediments of Park Hill deflects the contours of the local anomaly (figure 6) in the vicinity of Park Hill. They would be deflected a slight (less than 0.3 milligal) additional amount if the terrain correction had not been ignored.

SEISMIC SURVEY

To determine more accurately the depth of valley filling sediments in the San Jacinto valley, a seismic refraction survey was conducted.

The seismic velocity of granitic bedrock in the area of investigation was first determined. This was accomplished by Dr. Eaton, University of California at Riverside (UCR) students, and the writer with the writer's Texas Instrument EXPLORER system. Measurements were made on the northeast side of the Lakeview mountains, both across foliation and along foliation. The rock was found to be anisotropic, with minimum velocity about 14,500 feet per second across foliation and maximum velocity about 17,000 feet per second along foliation.

On two commercial seismic investigations in the area, the writer measured the seismic velocity of unweathered metamorphic bedrock and found 15,000 to 16,000 feet per second to be typical. The metamorphics displayed less anisotropy than the foliated granitics.

Line A

The first line profile, Line A, figure 7, was located along the axis of the gravity low with the city of San Jacinto at the center of the line.

Drs. Shawn Biehler and Stewart Smith of the California Institute of Technology, Dr. Gordon Eaton of UCR, students of both schools, and the writer performed the recording of Line

FIGURE 7

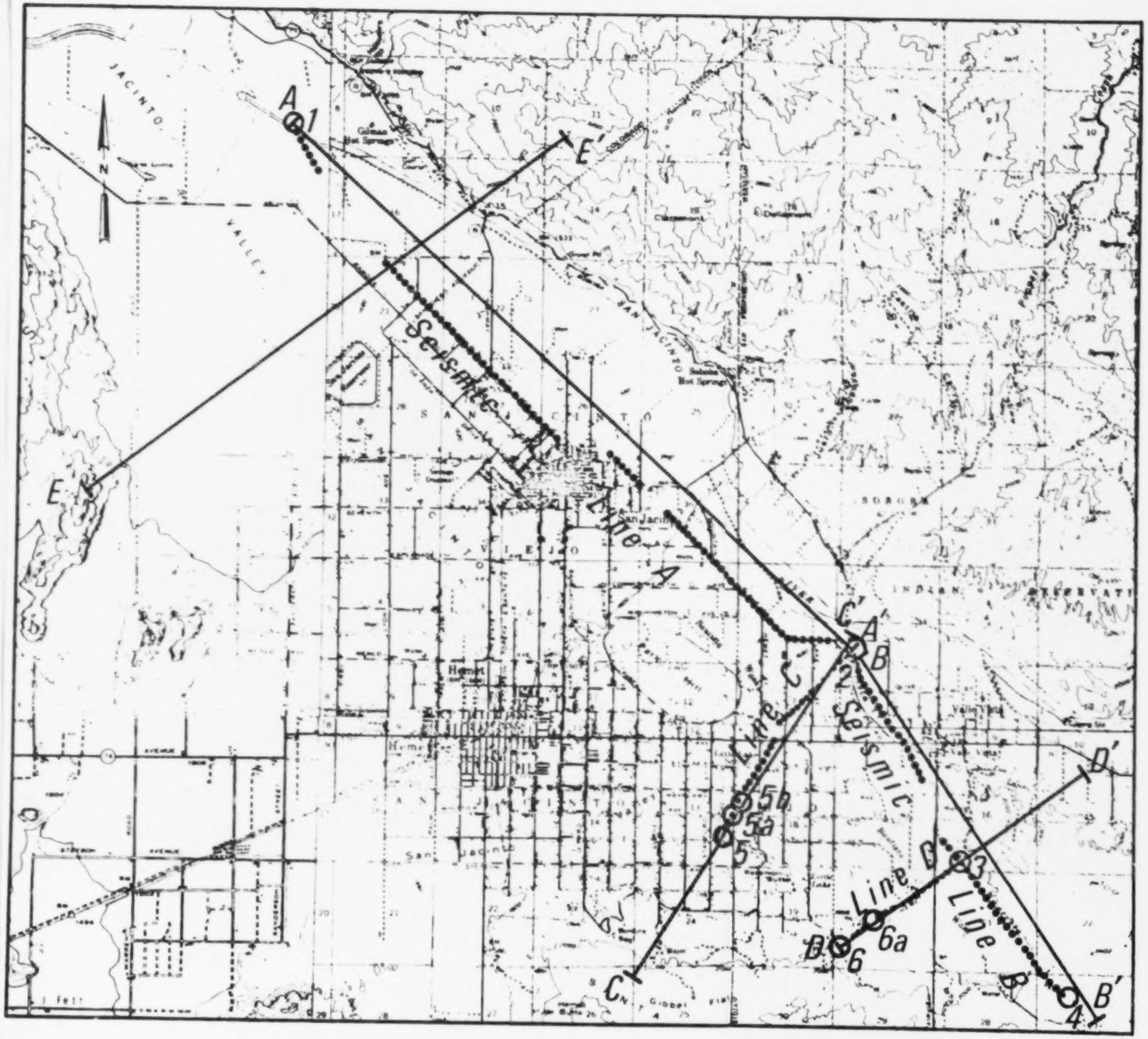
A
1
E'
E
JACINTO
VALLEY
N
Seismic
Line A
SAN JACINTO
C'
A
B
2
Seismic
Line C
5b
5a
5
C
D'
3
Line D
6a
D
6
Line B
B'
4
E — E'
Geologic Section
Seismic Line
○6
Shot Point
ONE MILE

NOT REPRODUCIBLE

Locations of Geologic Sections, Seismic Lines, and Shot Points

A data from Shot Point 1. The shot point was at the northwest end of the line and was located in the San Jacinto river bed just west of the junction of Massacre Canyon creek with the river. The location of this shot point and the recording locations are plotted on figure 7. California Institute of Technology (CIT) personnel supervised operations at Shot Point 1. Shot instant was radioed to recording units by CIT's tone generating blaster. Several seconds before shot time a 400 Hz tone was transmitted. This tone was interrupted at the precise instant of cap detonation. The tone signal was received at recording units and placed on records by auxiliary galvanometers.

Eastern Municipal Water District (EMWD) supplied explosives and the men and equipment to place the charges for all seismic work. Dynamite was used for the explosive agent for Shot Point 1. Charge size increased as recording locations became more distant. Maximum shot size was a little in excess of 500 pounds.

To verify the findings of the above work and to determine the dip of the bedrock, Line A was reversed. The reversal was performed by Dr. Eaton and the writer, with the aid of UCR students. The writer's TI EXPLORER seismic equipment and tone blaster together with EMWD radio equipment were used for the reversal of Line A and all subsequent work.

The shot point, Shot Point 2, was at the southeast end of the line, in Bautista creek, just north of Cedar avenue.

The location of Shot Point 2 is plotted on figure 7.

To economize on explosive costs, the writer instructed EMWD personnel in the use of ammonium nitrate - fuel oil explosive. This reduced explosive costs to about 18 percent that of conventional explosive.

Shot holes were dug with a back-hoe and the hole depth was limited to about 11 feet. To increase the efficiency of the explosive charges, no more than 120 pounds were placed in a single shot hole. When larger charges were needed, they were obtained by connecting two or more shot holes together with Primacord detonating fuse. Thus, more energy went into seismic wave generation and less into the air. This also had the effect of keeping the predominant frequency of the seismic pulse close to that desired for optimum transmission and recording. Cratering was also reduced. Subsequent to this field work, O'Brien (1967) published information on the efficient use of large charges.

Distance and travel-time data of Line A are tabulated in the appendix and plotted on figure 8.

Line A Interpretation

CIT interpreted the unreversed data of Line A from Shot Point 1. The water table was interpreted to be 30 feet below the surface near Shot Point 1. The seismic velocity of the unsaturated sediments was 1,300 feet per second and the saturated sediments beneath the water table had a velocity of

FIGURE 8

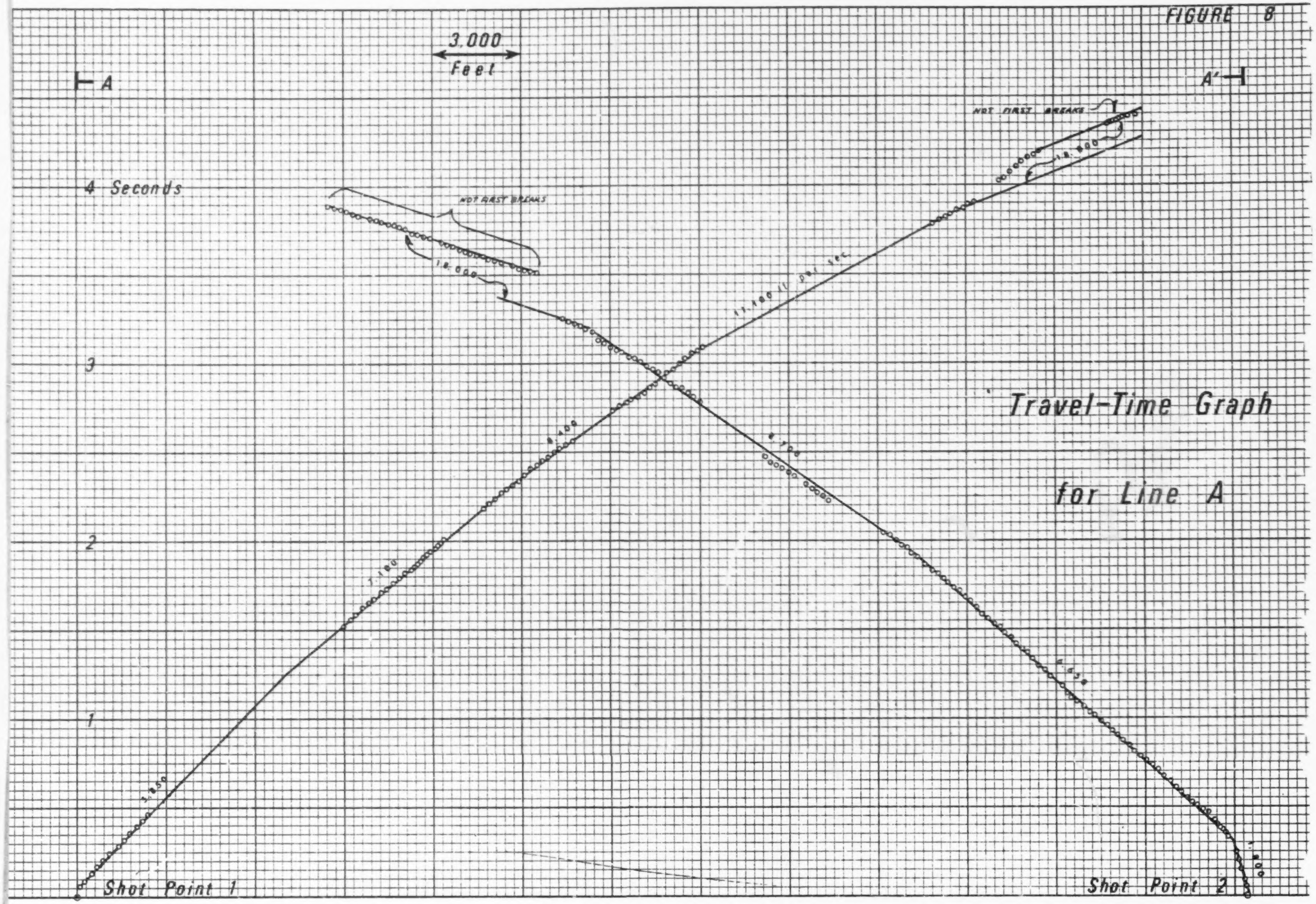

Travel-Time Graph for Line A

5,500 feet per second. The velocity was interpreted as increasing to 7,350 feet per second at a depth of 830 feet. At a depth of 1,920 feet the velocity increased to 8,650 feet per second and at a depth of 5,400 feet it was interpreted as increasing to 10,150 feet per second. The bedrock was interpreted to be 10,400 feet beneath San Jacinto. There were no travel-time data recorded between 21,100 and 28,900 feet from Shot Point 1. The critical distance for the bedrock refraction appears to be about 29,700 feet from Shot Point 1. Figure 9 is the seismic recording on which the bedrock refraction appears to become the first arrival. There is some uncertainty in the above interpretation because of the lack of data along almost a mile and a half of line and because of the possibility of the change in apparent velocity at 29,700 feet from Shot Point 1 being caused by irregularity of the water table. There are several large production water wells in the area east and southeast of San Jacinto.

The writer's interpretation of the unreversed Line A data from Shot Point 2 places the water table, in the vicinity of Shot Point 2, at a depth of about 200 feet. At a depth of about 2,200 feet a mile northwest of Shot Point 2, the velocity of the sediments increases to about 8,700 feet per second. The bedrock surface is about 7,800 feet beneath Line A approximately two miles northwest of Shot Point 2. These depths are based on a four layer model with velocities of 1,800, 6,650, 8,700 and 18,000 feet per second and critical

FIGURE 9

SEISMIC RECORD CIT-V, LINE A, SHOT POINT 1

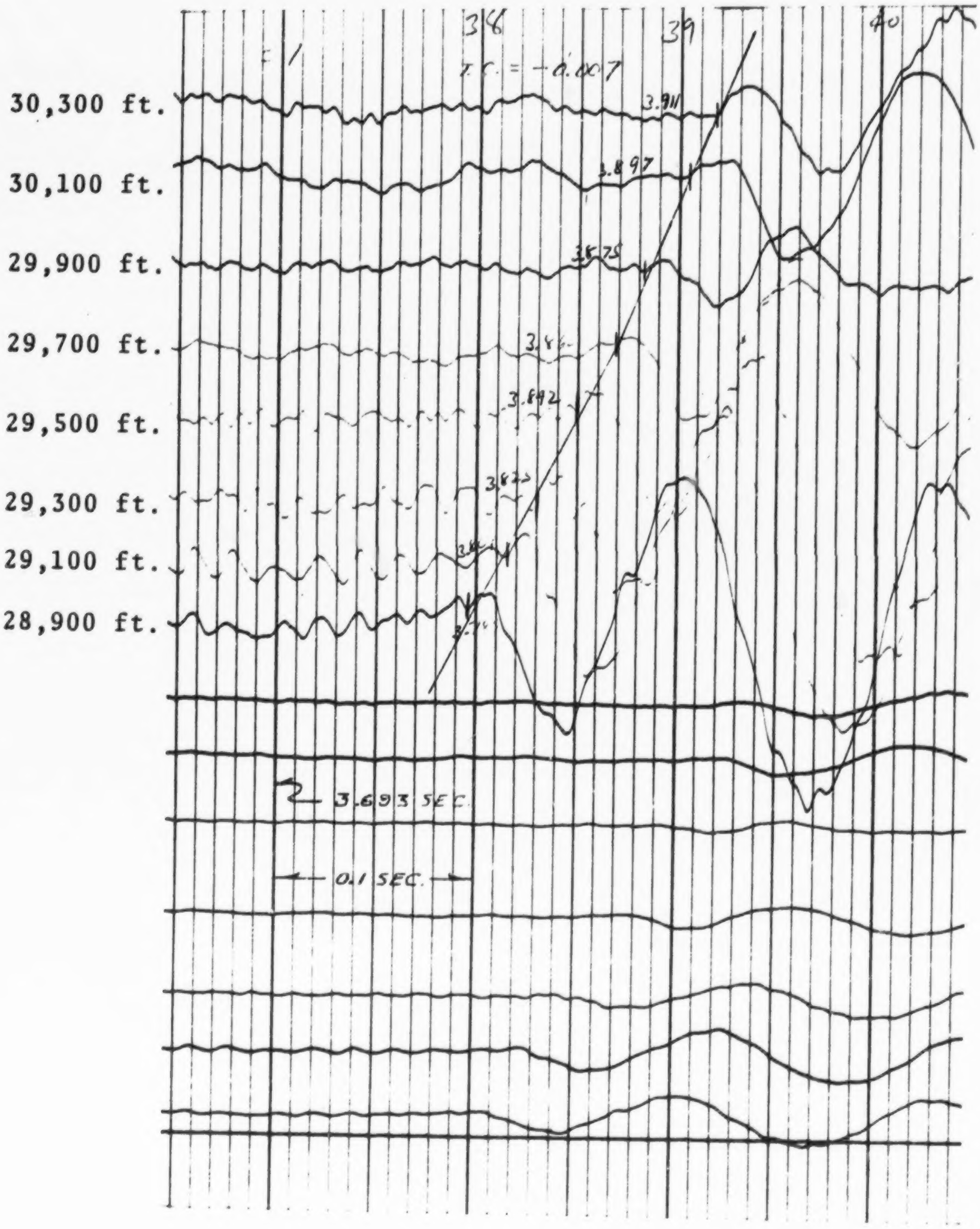

distances of 550, 11,300, and 22,200 feet. Figure 10 is the seismic recording on which the bedrock refraction becomes the first arrival.

It seems likely that the 8,700 feet per second surface at a depth of 2,200 feet is the same surface as the 8,650 feet per second surface calculated by CIT to be at a depth of 1,920 feet approximately a mile and a half southeast of Shot Point 1. There are four and a half miles between these depth determinations. Since the elevation of Shot Point 2 is approximately 220 feet greater than that of Shot Point 1, the average dip of this surface between the depth determinations is approximately zero.

The two bedrock depth determinations are horizontally separated by about two and a half miles and the northeasterly determination is approximately two and a half thousand feet deeper than the southeasterly determination. A northwesterly dip of about 12 degrees could be inferred, but the recorded apparent bedrock velocities do not tend to confirm a northwesterly dip. The apparent bedrock velocity of 18,000 feet per second, from Shot Point 2, is rather well established. The apparent bedrock velocity from Shot Point 1 is not clearly determined. Line A at least indicates a minimum depth of about 8,000 feet beneath San Jacinto. Additional recording from Shot Point 1 to the southeasterly portion of Line A should clarify the above findings. There is a possibility that the bedrock refractions from Shot Point 1 are refractions

FIGURE 10

SEISMIC RECORD 8, LINE A, SHOT POINT 2

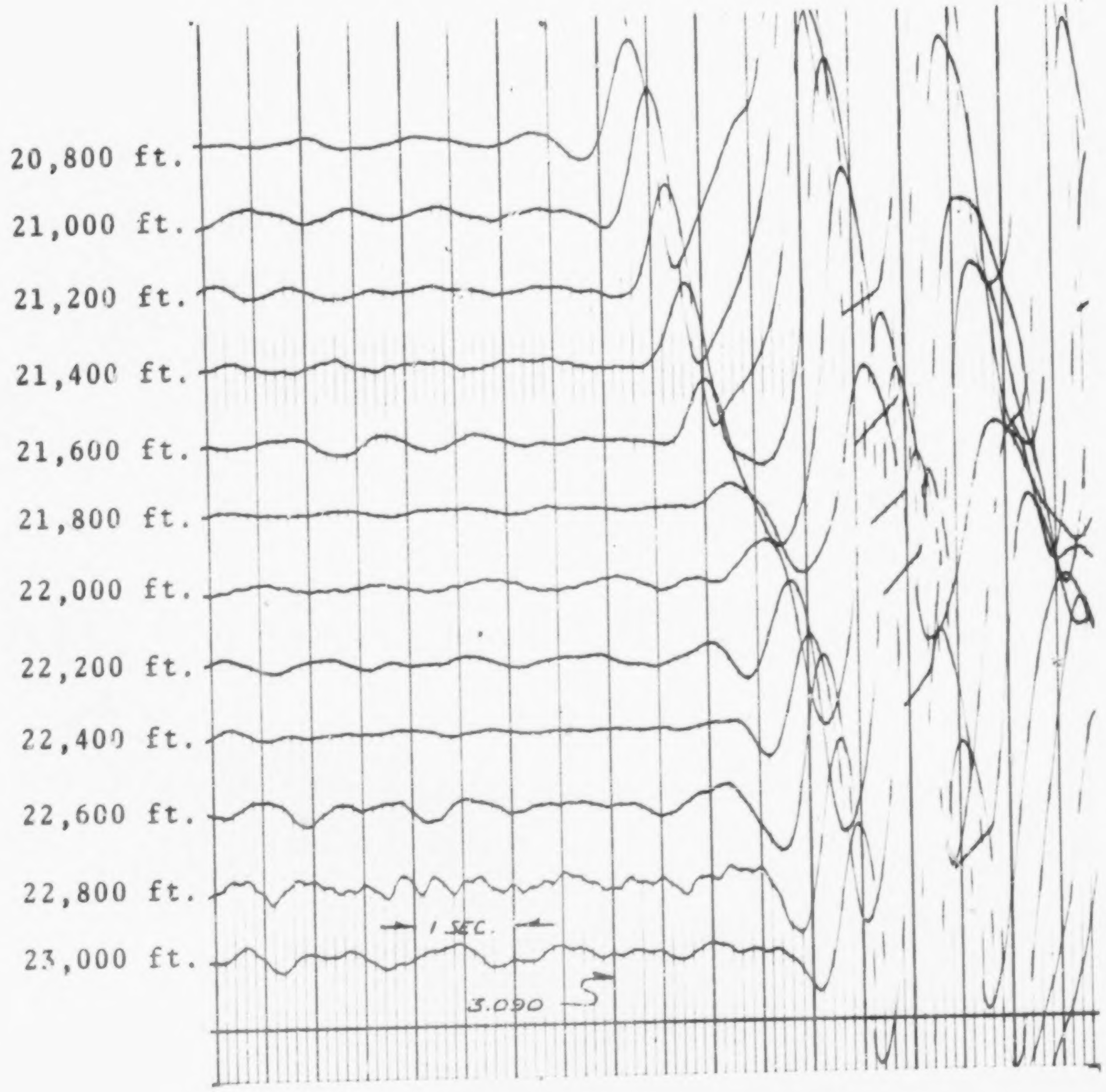

from the side of the graben. The seismic interpretations are based on the assumptions that there are no hidden layers (Green, 1962) or velocity reversals. A perched water table in the vicinity of Shot Point 1 would tend to make the deeper refractors appear excessivly deep.

Having velocity information from the refraction work, reflection recording in the San Jacinto valley should now be more feasible.

Line B

With the assistance of EMWD, the writer performed three more deep seismic profiles in the upper portion of the San Jacinto valley.

Line B follows the Bautista creek - Bautista flood control channel from Shot Point 2, near the junction of Bautista creek with the San Jacinto river, through-Shot Point 3, to Shot Point 4 at the mouth of Bautista canyon. The locations of Line B and Shot Points 2, 3, and 4 are plotted on figure 7. Except for Shot Point 2, size of charges was limited by cultural development. The distance and travel-time data are tabulated in the appendix and plotted on figure 11.

Line B Interpretation

Near the northwest end of Line B, the seismic data indicate a water table at a depth of 195 feet. A refractor of higher seismic velocity is indicated at a depth of approximately 485 feet beneath Line B, a quarter of a mile north-

FIGURE 11

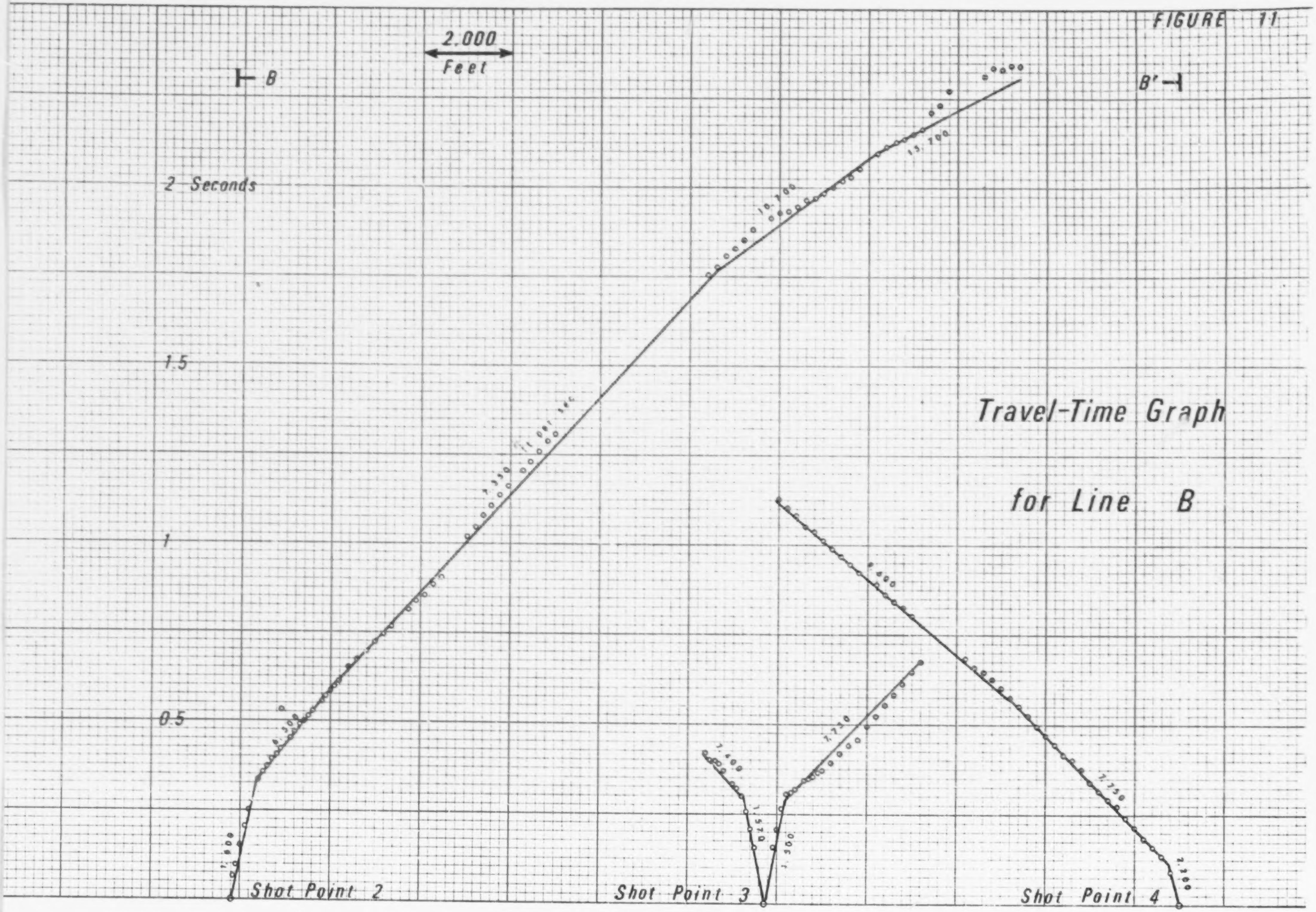

Travel-Time Graph for Line B

east of Shot Point 2. These depths are based on a three layer model with velocities of 1,600, 6,500, and 7,350 feet per second and critical distances of 500 and 2,400 feet.

Shot Point 3 is near the center of Line B. A few hundred feet northwest of Shot Point 3, the seismic data indicate the water table to be at a depth of 182 feet. This depth is based on a two layer model with velocities of 1,570 and 7,400 feet per second and a critical distance of 450 feet. A few hundred feet southeast of Shot Point 3, the seismic data indicate a water table at a depth of 185 feet. This depth is based on a two layer model with velocities of 1,500 and 7,750 feet per second and critical distance of 450 feet.

Near the southeast end of Line B, the seismic data indicate the water table to be at a depth of about 100 feet beneath the down-stream base of the Riverside County Flood Control dam. This portion of the seismic field work was performed in late April, 1967, and water depth behind the dam was about four feet. It is likely that the water table rapidly increased in depth to the northwest, (down-valley). The seismic data from Shot Point 4 also indicate a refractor with an apparent velocity of 9,600 feet per second at a depth of 660 feet below Line B about midway between Shot Points 3 and 4. These depths are based on a three layer model with velocities of 2,200, 7,750, and 9,600 feet per second and critical distances of 250 and 3,600 feet.

The seismic data of Line B do not yield clear and precise information on the depth to bedrock. It is likely that a bedrock refraction from Shot Point 2 becomes a first arrival at about 14,000 feet from Shot Point 2. Figure 12 is the seismic recording on which the bedrock refraction appears to become the first arrival. The depth to this refractor is approximately 4,700 feet beneath the middle of Line B. This depth is based on a five layer model with velocities of 1,600, 6,500, 7,350, 10,700, and 15,700 feet per second and critical distances of 500, 2,400, 10,700, and 14,400 feet. This refraction may be a side refraction from the bedrock face of the San Jacinto - Bautista Creek fault. The bedrock depth beneath the middle of Line B is a minimum of 4,700 feet.

Line C

Lines C and D are at right angles to the predominant trend of faulting in the valley.

Line C is located between Shot Point 2 and Shot Point 5. Shot Point 5 is about two and a quarter miles southwest of Shot Point 2. Observations along the southwest portion of Line C were supplemented by two small shots, Shot Points 5a and 5b. The locations of these shot points and Line C are plotted on figure 7. Distance and travel-time data are tabulated in the appendix and plotted on figure 13.

Line C Interpretation

Near the northeast end of Line C, the seismic data indicate a water table at a depth of approximately 210 feet. This depth to the water table is consistent with Line A and B

FIGURE 12

SEISMIC RECORD 6, LINE B, SHOT POINT 2

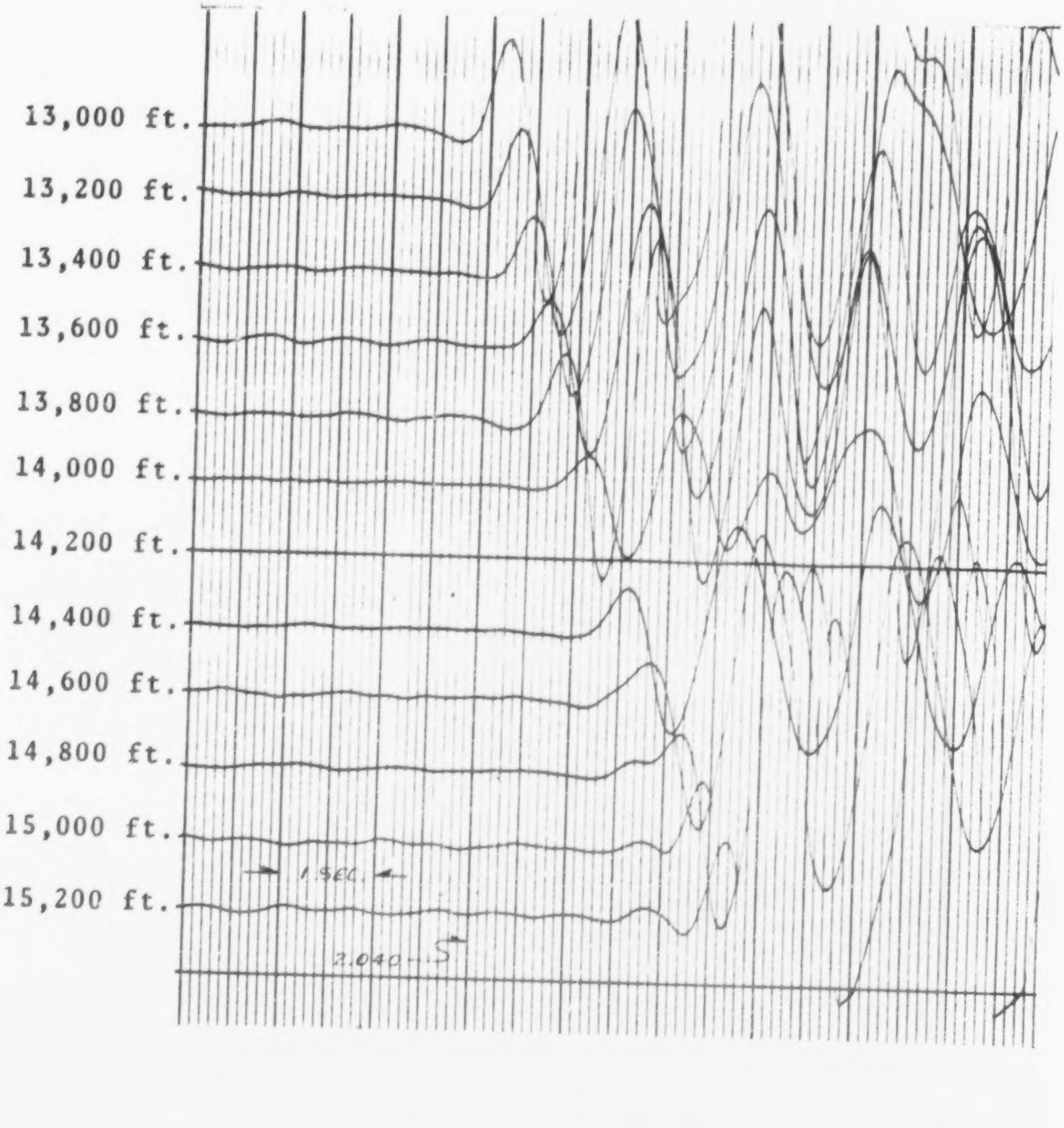

FIGURE 13

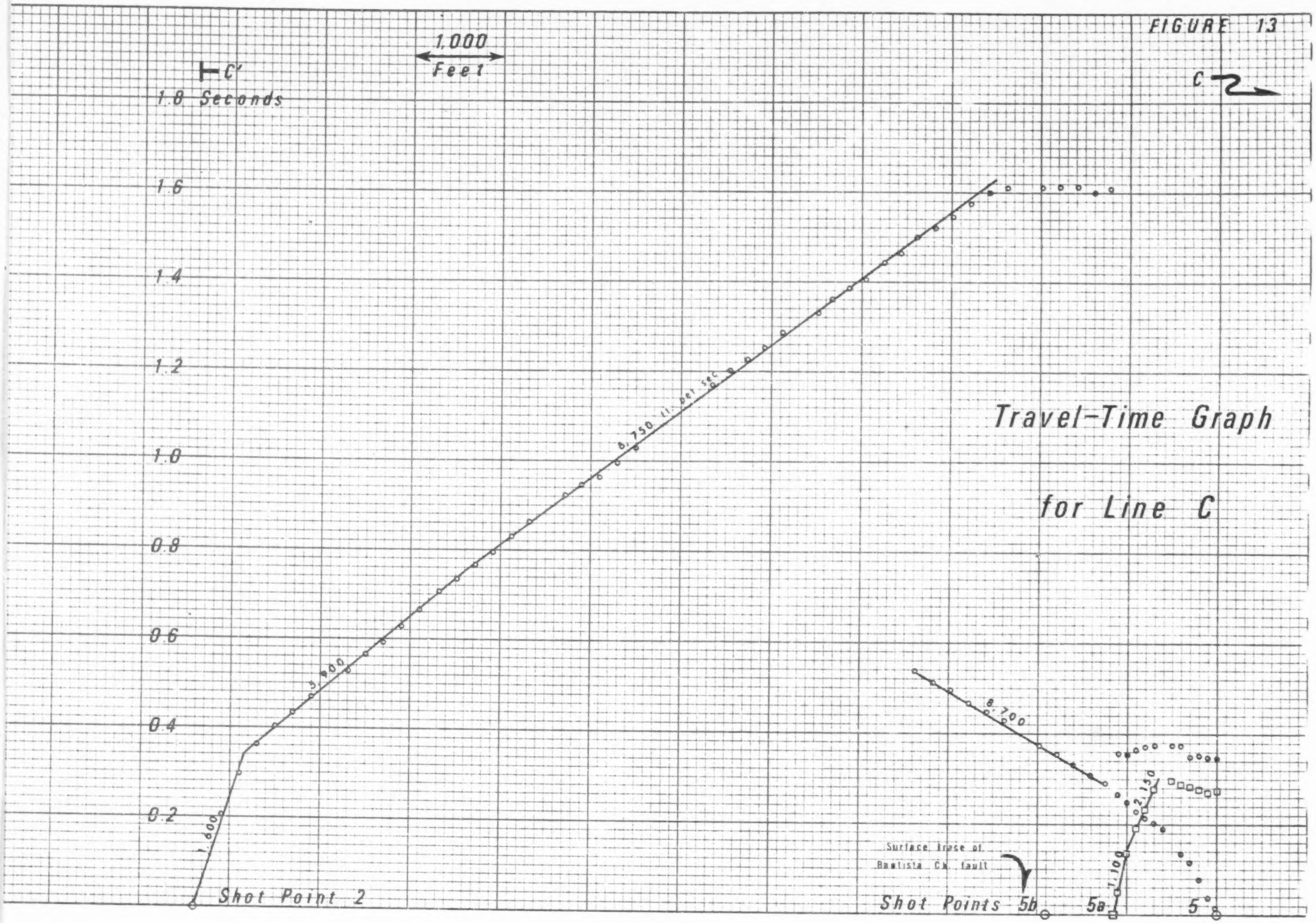

Travel-Time Graph

for Line C

data and an observation of 199 feet, made a month prior to the seismic field work, in a test hole about 600 feet west-southwest of Shot Point 2.

A refractor of higher seismic velocity is indicated at a depth of approximately 580 feet beneath Line C, a quarter of a mile southwest of Shot Point 2. The above mentioned test hole encountered boulders from a depth of 528 feet to approximately 580 feet. Below this depth, the hole penetrated fine grained clastics and bottomed in these fine grained clastics at a depth of 800 feet. It seems likely that these fine grained sediments are part of the Bautista Formation or younger Pleistocene sediments and a conglomerate was deposited on their erosional surface.

From Shot Point 2, no refraction from bedrock is observed until the Bautista Creek fault is approached. This is a distance of about 9,000 feet. If the bedrock beneath this segment of Line C has zero dip, the depth to bedrock would be in excess of 3,200 feet. This minimum depth seems consistent with both the geology and seismic Lines A and B.

These depths are based on a four layer model with velocities of 1,600, 5,900, 6,750, and 16,000 feet per second and critical distances of 550, 3,000, and 9,000 feet.

Near the southwest end of Line C, first arrivals from Shot Point 2 have an approximately infinite apparent velocity. One solution that would explain these arrivals and the seismic information from Shot Point 5, and be consistent with the geology is the following: waves from Shot Point 2, upon reaching the Bautista Creek fault, would be refracted up the bedrock face of the fault and then diffracted. The diffracted waves would radiate in all directions. Some would pass up through saturated sediments, be refracted at the water table and emerge, almost simultaneously, along a few hundred feet of Line C, to each side of the fault.

From the fault, the bedrock surface becomes shallower until it crops out at Shot Point 5. About 700 feet northeast of Shot Point 5, the data from Shot Point 5a indicate bedrock depth to be approximately 250 feet. A little further to the northeast, the sediment depth becomes sufficient for the water table to be encountered. From the water table to the fault, the bedrock surface must dip to the northeast at an angle of about 20 to 25 degrees to account for the low apparent velocity recorded from Shot Point 5. At the fault, the bedrock depth is approximately 800 feet.

The available data could also be explained without a fault. This alternate solution would be a bedrock surface dipping to the northeast at an angle of about 22 degrees. This dip would account for both the infinite apparent velocity at the southwest end of Line C from Shot Point 2 and the apparent velocity of 8,700 feet per second from Shot Point 5. This dip calculation is based on a bedrock velocity of approximately 16,000 feet per second and a saturated sediment velocity of approximately 6,000 feet per second.

Though the alternate solution also fits the seismic data of Line C, it does not seem a likely solution from the geologic point of view. The question could be resolved by extending the seismic recording from Shot Point 5 further to the northeast or by reflection recording a quarter of a mile northeast of the Bautista Creek fault.

Line D

Line D extends along the Lake Hemet Municipal Water District's flume from Bautista flood control channel, at Shot Point 3, to Shot Point 6, which is located on bedrock about a mile southwest of Shot Point 3. Observations along most of Line D were supplemented by shots in the small reservoir near the center of section 20, (Shot Point 6a). The locations of Line D and these shot points are plotted on figure 7. The distance and travel-time data are tabulated in the appendix and plotted on figure 14.

Line D Interpretation

A 1,300 foot spread was recorded from Shot Point 3 to the northeast. It indicated a water table at a little over 200 feet and a higher velocity refractor, probably the Bautista Formation, shoaling to the northeast. The water table depth is based on a three layer model with velocities of 1,250, 2,100, and 6,800 feet per second and critical distances of 200 and 500 feet.

To the southwest, seismic data from Shot Point 3 indicate refractors at depth of 115, 360, and 590 feet. Nearby

FIGURE 14

Travel-Time Graph for Line D

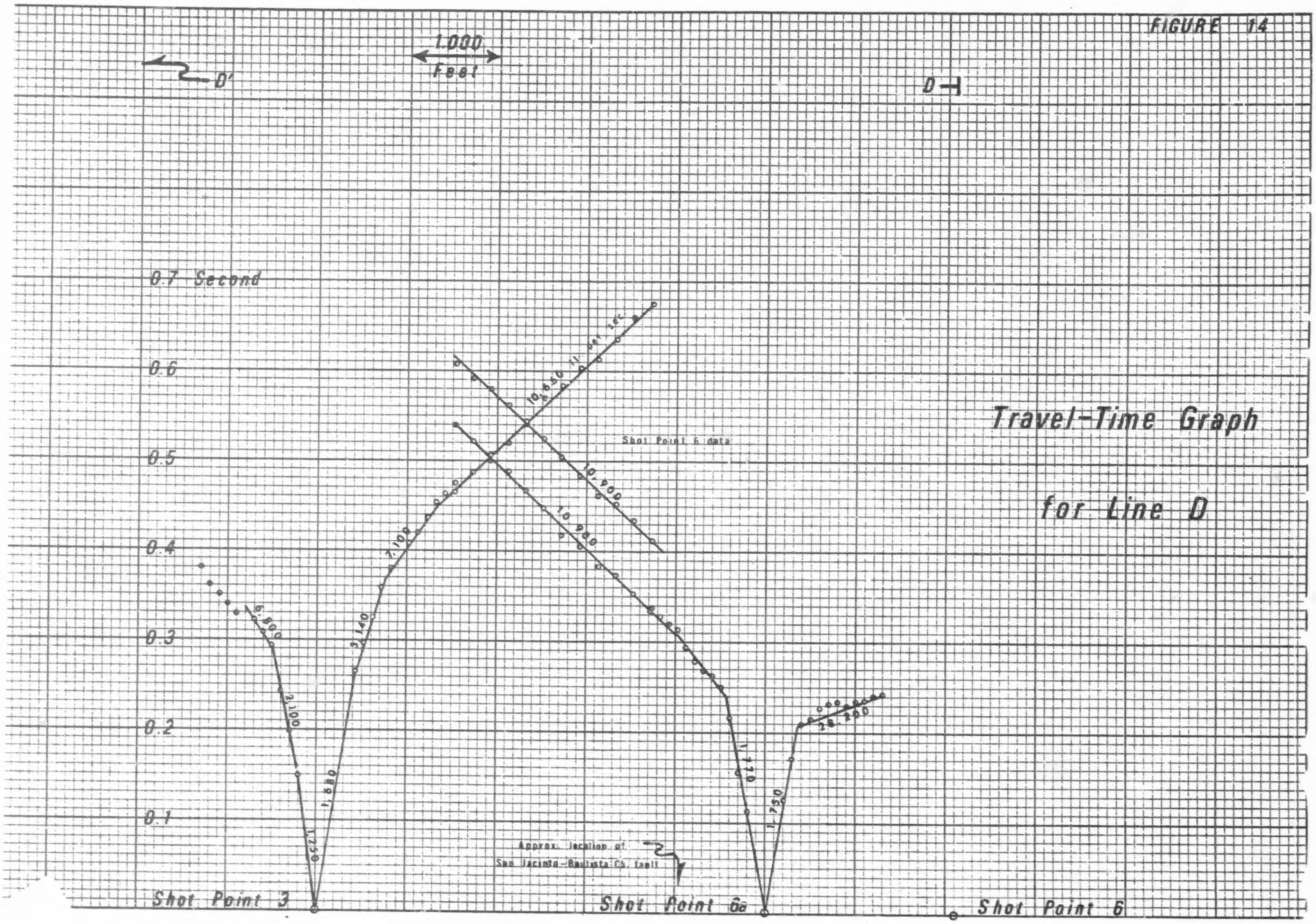

agricultural water wells cause irregularities in the water table beneath Line D, which in turn make the interpretation of the shallower refractors subject to substantial error. The 10,660 feet per second refractor at a depth of 590 feet is undoubtedly the surface of the Bautista Formation. Assuming a zero dip bedrock of 16,000 feet per second seismic velocity, its minimum depth would be about 1,350 feet. These depths are based on a five layer model with velocities of 1,680, 3,140, 7,100, 10,660, and 16,000 feet per second and critical distances of 420, 870, 1,320, and 3,700 feet.

A few hundred feet southwest of Shot Point 6a, the seismic data from Shot Point 6a indicate bedrock to be at a depth of about 150 feet and shoaling to the southwest with an apparent dip of about 10 degrees. This depth and dip are based on a two layer model with a critical distance of 350 feet, a surface layer velocity of 1,750 feet per second and apparent and assumed true bedrock velocities of 28,200 and 16,000 feet per second, respectively.

To the northeast of Shot Point 6a, the seismic data indicate the water table at a depth of approximately 170 feet and a 10,900 feet per second refractor at a depth of about 350 feet. It is likely that the 10,900 feet per second refractor is the surface of the Bautista Formation. Since the bedrock surface is two to three hundred feet beneath Shot Point 6a, the seismic waves from Shot Point 6a passed through several hundred feet of bedrock until reaching the

San Jacinto-Bautista Creek fault, then refracted from the surface of the Bautista Formation. Correcting for the bedrock portion of the refracted wave's path, the surface of the Bautista Formation is probably at a depth of about 500 to 600 feet on the northeast side of the fault. The information from Shot Point 6 tends to confirm this interpretation.

FINDINGS AND THEIR IMPLICATIONS

The gravity survey has determined, in a qualitative manner, the bedrock topography to the southwest of Casa Loma fault. The Bouguer anomaly with the regional removed, figure 6, shows good correlation between the magnitude of the local Bouguer gravity anomaly and bedrock depths obtained from well log information, figure 3. Based on well log information, seismic information, and mostly gravity information, the drainage patterns on the buried bedrock surface have been plotted on figure 15.

With the detailed processing and interpretation of this and Dr. Eaton's gravity data, it will be possible to plot quantitatively the bedrock elevation.

Knowledge of bedrock configuration beneath the valley fill on the Hemet side of the Casa Loma fault is of prime importance for an understanding of ground water in the area. Wells with optimum specific capacity may be expected to occur where drilled to bedrock along the buried drainage courses on the bedrock surface. In these locations the sediments just above bedrock should be coarser grained than those just above the higher slopes or ridges of the bedrock.

The City of Hemet well near Stetson avenue and Gilbert street is an example of this principle. It is located near a trough in the gravity anomaly, and is quite probably located over the channel in the bedrock surface that drained

FIGURE 15

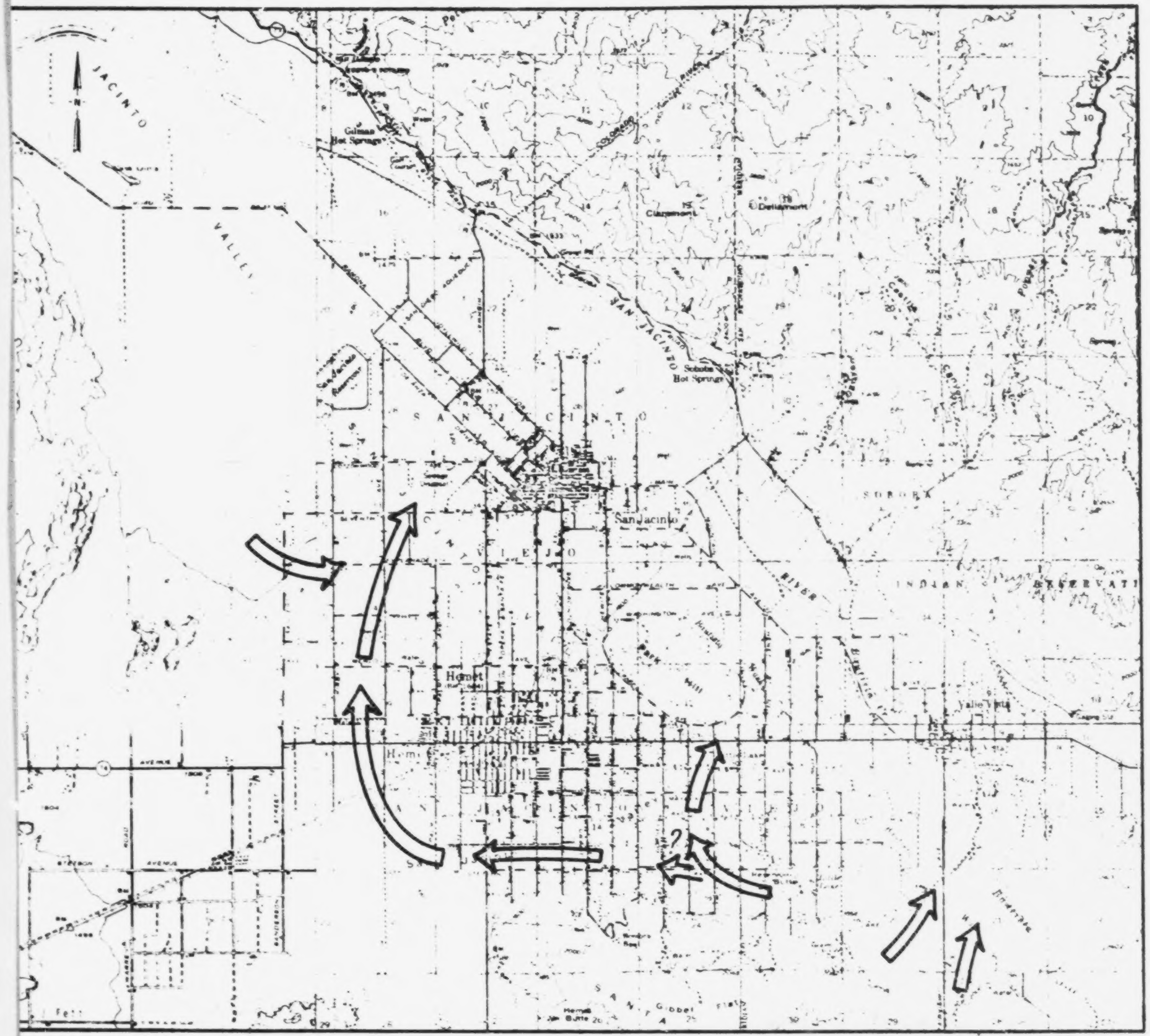
JACINTO
VALLEY
Gilman Hot Springs
SAN JACINTO
Soboba Hot Springs
SAN JACINTO
San Jacinto
SOBOBA
INDIAN RESERVATI
RIVER
Hemet
Valle Vista
?

Drainage Patterns
on the
Buried Bedrock Surface

ONE MILE

from the east, passing beneath this well site, then turned northward. The well passes through coarser grained sediments, predominently subrounded fine gravel and coarse sand, in the one hundred and fifty feet immediately above bedrock. The specific capacity of the well is excellent and should remain good even if the water table is lowered, since the major zone of production is in the lowest portion of the well.

Though there are few bedrock outcrops between the Casa Loma fault and the hills on the south of the San Jacinto valley, prolonged overdraft of the valley's ground water has lowered the water table sufficiently for many buried bedrock hills and ridges to form "islands" and "peninsulas" rising above the water table, but not above the surface of the sediments. The area southeast of Florida avenue and San Jacinto street is such a region.

As a result of the many barriers formed by the irregular surface of the buried bedrock, a well of good specific capacity may lower the water table in its vicinity an abnormal amount if the well is located in an alcove and cut off on several sides by such barriers. If the water table continues to decline, these barriers become increasingly important in the prediction of the long term potential of a well site. The buried drainage courses on the bedrock surface become increasingly important in the location of wells of sufficient yield to be economical sources of water supply.

Based on the interpretation of the seismic data, and available subsurface information, five geologic cross sections of the valley have been constructed. The locations of the geologic sections are plotted on figure 7. The sections constitute figures 16 through 19. Figure 20 is a block diagram of the San Jacinto valley area.

Geologic Sections A, figure 16, is approximately along the alignment of seismic Line A. The depth to bedrock beneath San Jacinto is about 8,000 or more feet. The San Jacinto fault zone has dropped a wedge of bedrock, between the Claremont fault on the northeast side of the valley, and the Casa Loma fault that passes through the center of the valley. The writer suggests the name San Jacinto graben for this rift. The graben is continuing to increase in depth, as is indicated by the recentness of faulting on both the Casa Loma and Claremont faults. The dip of these faults is unknown. Near the surface, Proctor (1962) and Buwalda (Bean, 1955) observed a northeasterly dip of the Casa Loma fault in the unconsolidated Recent sediments. Most of the faults encountered near the Claremont fault in the San Jacinto tunnel of the Colorado River aqueduct dip steeply toward the northeast. If the 8,650-8,700 feet per second refractor of Line A represents the erosional surface of the Bautista Formation, this surface is about 2,000 feet deep through most of Section A.

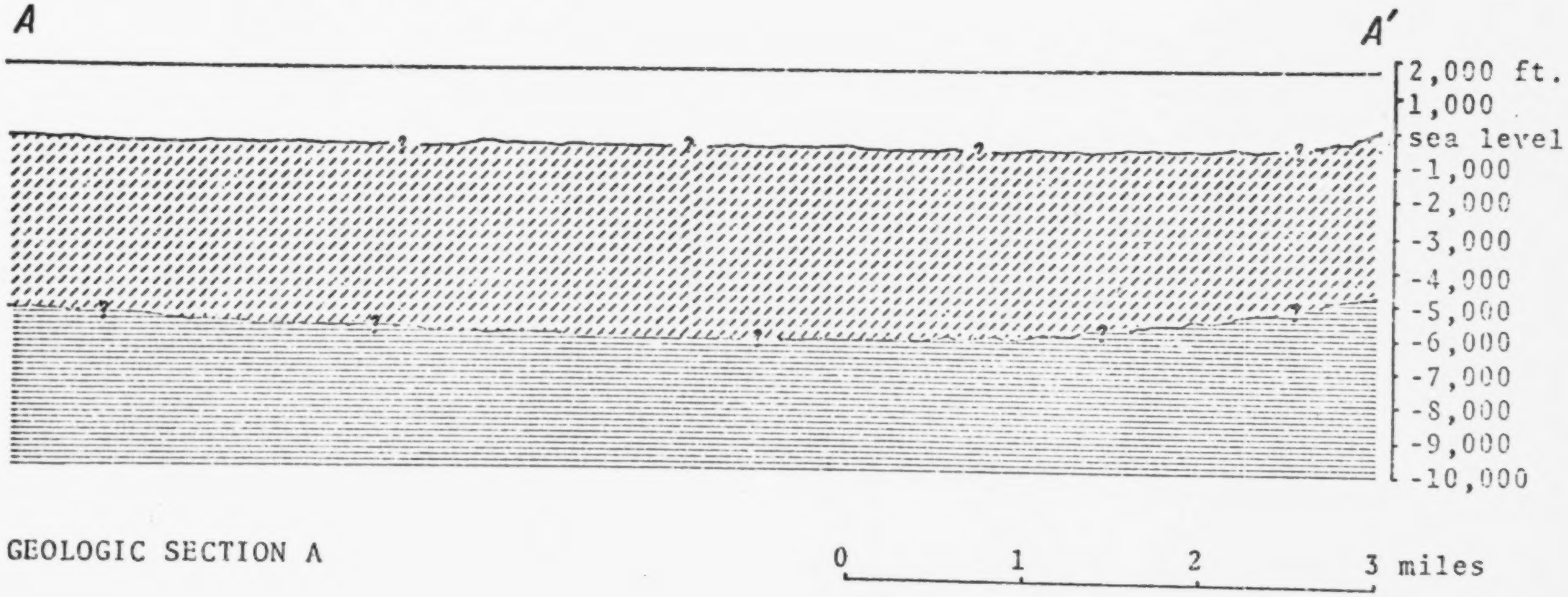
A
A′
2,000 ft.
1,000
sea level
-1,000
-2,000
-3,000
-4,000
-5,000
-6,000
-7,000
-8,000
-9,000
-10,000
?
0
1
2
3 miles

GEOLOGIC SECTION A

Key, symbols, and scale same as figure 2

FIGURE 16

Geologic Section B, figure 17, is approximately along the alignment of seismic Line B. The depth to bedrock at the center of this section is at least 4,700 feet and may be deeper if the refraction from bedrock is a side refraction from the bedrock face of the San Jacinto - Bautista Creek fault. The erosional surface of the Bautista Formation is probably at a depth of about 500 feet near the northwest end of Section B and crops out along the southeastern portion of this geologic section.

Geologic Section C, figure 18, is along the seismic Line C alignment and also extended to the southwest. At the center of this section is the Bautista Creek fault. There are a few feet of Recent vertical offset at the surface. On the southwest side of the fault, bedrock is at a depth of about 800 feet. On the northeast, bedrock depth is probably in excess of 3,000 feet, and may be much deeper.

Geologic Section D, figure 18, is along the alignment of seismic Line D. and extended to the northeast. From the hills south of the valley, the bedrock surface passes beneath the alluvium. At the San Jacinto - Bautista Creek fault, beneath the D alignment, the bedrock surface is at a depth of 400 to 600 feet on the southwest. On the northeast side of this fault, bedrock is in excess of 1,350 feet and probably deeper than 4,500 feet. The surface of the Bautista Formation reaches a maximum depth of about 550 feet between this fault

FIGURE 17

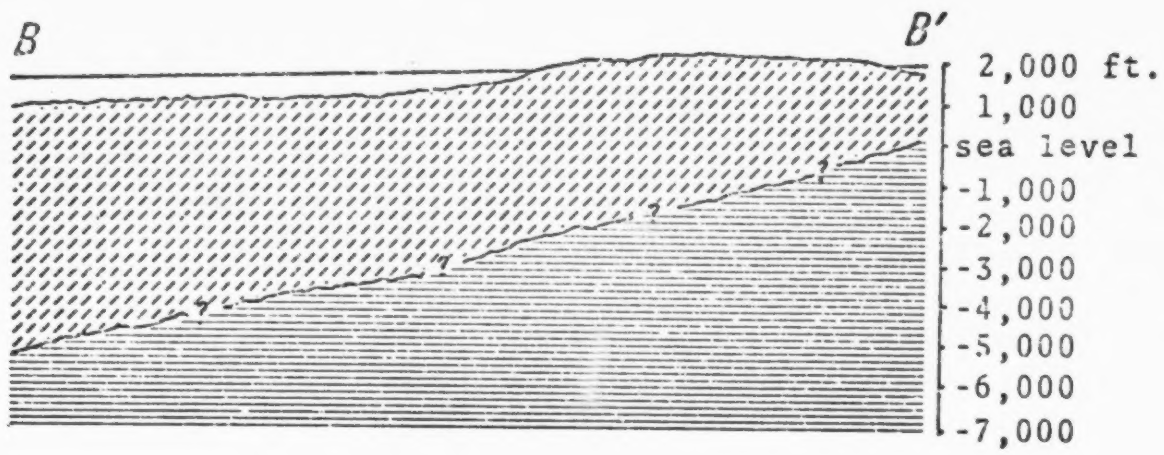
B
B'
2,000 ft.
1,000
sea level
-1,000
-2,000
-3,000
-4,000
-5,000
-6,000
-7,000

GEOLOGIC SECTION B 0 1 2 miles

Key, symbols, and scale same as figure 2

FIGURE 18

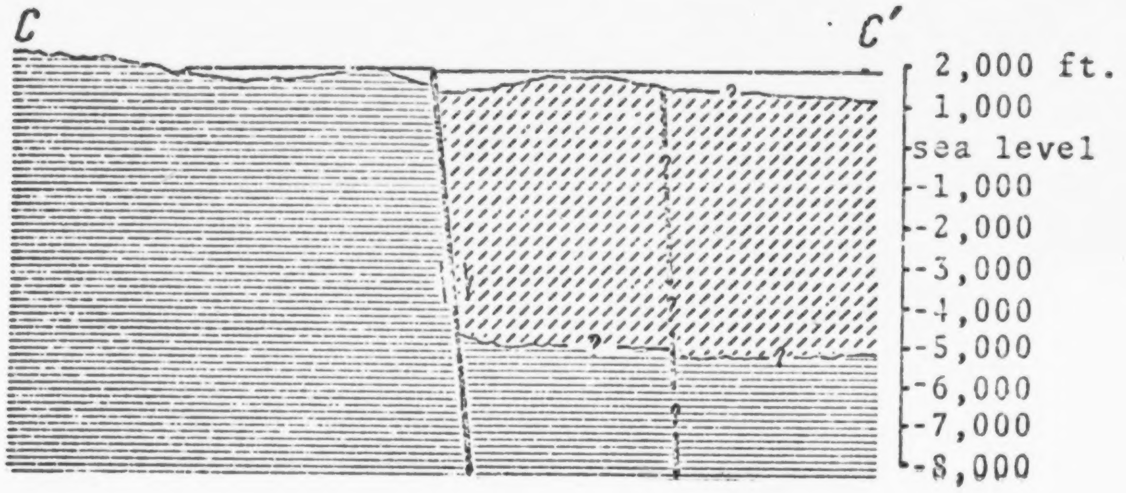
C
C′
2,000 ft.
1,000
sea level
-1,000
-2,000
-3,000
-4,000
-5,000
-6,000
-7,000
-8,000
?

GEOLOGIC SECTION C 0 1 mile

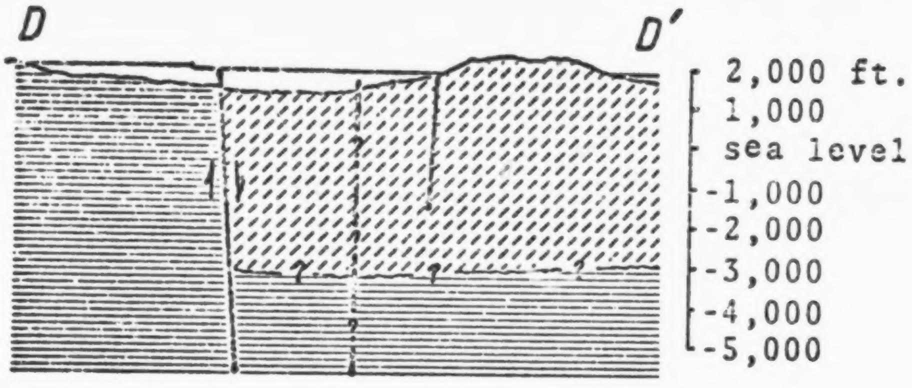
D
D′
2,000 ft.
1,000
sea level
-1,000
-2,000
-3,000
-4,000
-5,000
?

GEOLOGIC SECTION D 0 1 mile

Key, symbols, and scale same as figure 2 and the hills to the northeast, which are composed of Bautista Formation and capped, in places, with younger terrace forming sediments.

Geologic Section E, figure 19, is based partly on seismic work of Dr. Eaton and the writer. Southwest of the Casa Loma fault, a seismic line was performed along a portion of the alignment of Section E. This seismic work found the bedrock surface at a depth of about 380 feet midway between the Lakeview mountains and the Casa Loma fault. This bedrock depth increased to a depth of 500 to 600 feet near the Casa Loma fault (Eaton, personal communication). Bedrock depth northeast of the fault is probably 7,000 to 8,000 feet, based on seismic Line A information.

The San Jacinto fault enters the valley at the mouth of Bautista canyon, continues northwest under the name "Bautista Creek fault", and further northwest under the name "Casa Loma fault". Fault movement appears to have an increasingly greater dip-slip component toward the northwest. Perhaps some future confusion might be avoided if this fault would be called Casa Loma fault from the mouth of Bautista canyon to the northwest, and the San Jacinto fault to the southeast of the canyon mouth.

Sharp (1967) has mentioned that the San Jacinto fault zone has, in addition to many miles of right-lateral offset, considerable vertical offset, having dropped the area northeast with respect to that on the southwest. The same sense

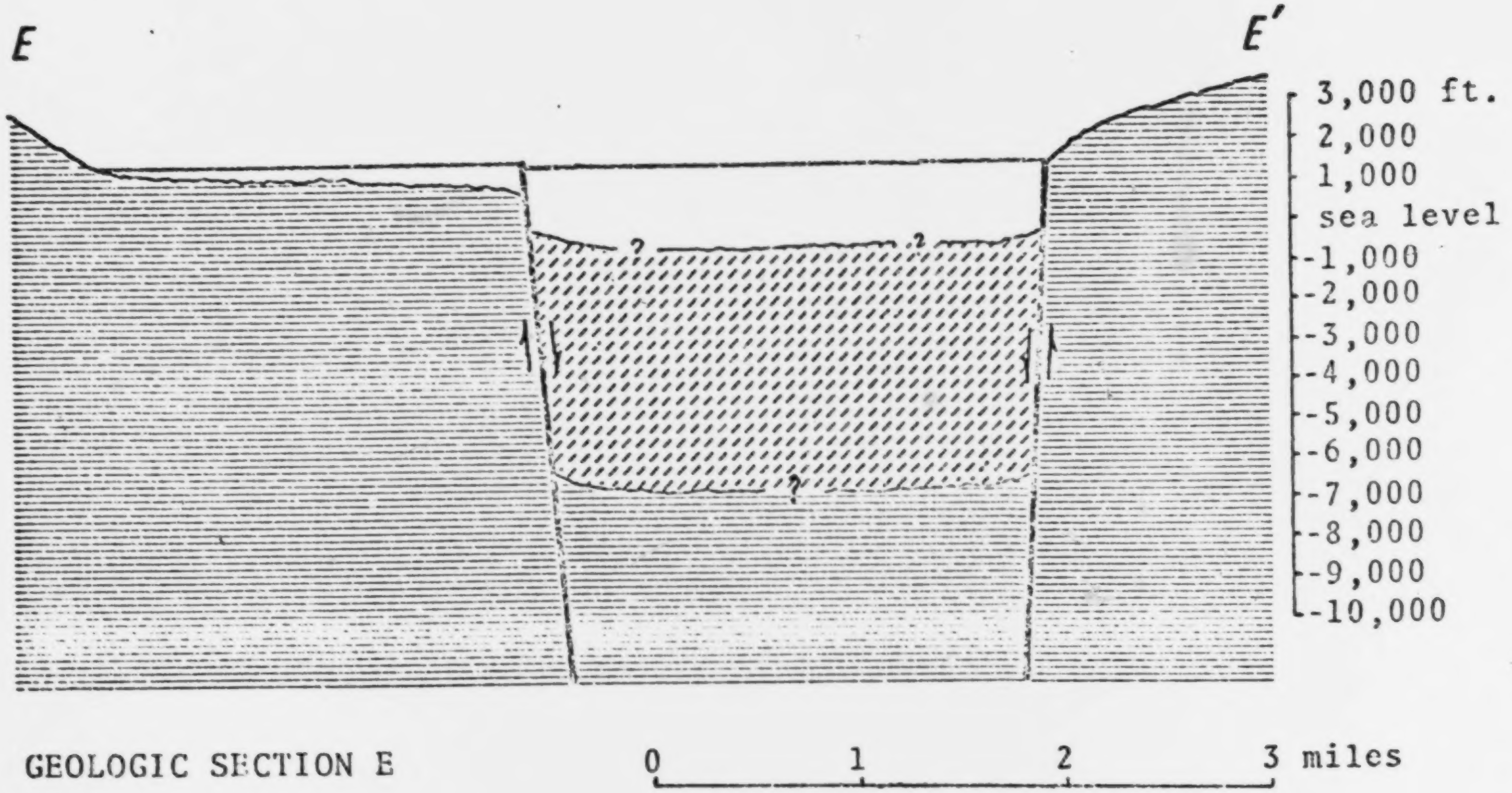
E
E'
?
?
?
3,000 ft.
2,000
1,000
sea level
-1,000
-2,000
-3,000
-4,000
-5,000
-6,000
-7,000
-8,000
-9,000
-10,000
0
1
2
3 miles

GEOLOGIC SECTION E

Key, symbols, and scale same as figure 2

FIGURE 19

of vertical movement is true of the Casa Loma fault.

Though the Casa Loma fault is less obtrusive in surface appearance than the Claremont fault, it is a major active fault. Because of its more subtle appearance, it is perhaps the more dangerous fault, for houses and structures, such as the San Jacinto reservoir, have been built along this fault. Its scarp has provided enough topographic relief to make attractive building sites.

Park Hill and Casa Loma are probably fault slivers. Geomorphic evidence suggests Park Hill to be bounded on its northeast by a fault, named the Park Hill fault. Though the existence of the Park Hill fault is most likely, the writer has not seen any definite evidence of its existence or non-existence.

Because of the activeness and size of the Casa Loma and Claremont faults, serious consideration and careful design should be used in structures and improvements near these faults. Both surface disruption and severe seismic vibrations are to be expected.

Future deep seismic investigation in the area can be performed with substantial savings in time and explosives if a greater number of recording channels are used and if the recording locations at greater distance from the shots or in areas of high background noise utilize multiple detectors for each channel. Recording during the early morning hours would also help avoid excessive background noise and reduce the minimum shot size required for a clear signal.

The gravity anomaly associated with the San Jacinto graben will be calculated and compared to the observed anomaly. Near the center of the graben the water table is at a depth of approximately 150 feet. The 1,920-2,200 foot refractor is assumed to be the surface of the Bautista Formation and an 8,000 foot depth to bedrock is used. In another part of the San Jacinto ground water basin, Eaton (personal communication) determined densities of 1.9, 2.3, and 2.7 for shallow unsaturated alluvium, shallow saturated alluvium, and granodiorite bedrock, respectively. From a depth of 1,000 feet to the surface of the Bautista Formation, a density of 2.4 seems reasonable because of the greater depth of burial (McCulloh, 1967). From the surface of the Bautista Formation to a depth of 5,000 feet, a density of 2.5 is assumed and from 5,000 feet to the bedrock surface, a density of 2.55 is assumed (McCulloh, 1967). Using these values, a 23.3 milligal anomaly is calculated. This is in close agreement with the observed anomaly of approximately 23 milligals.

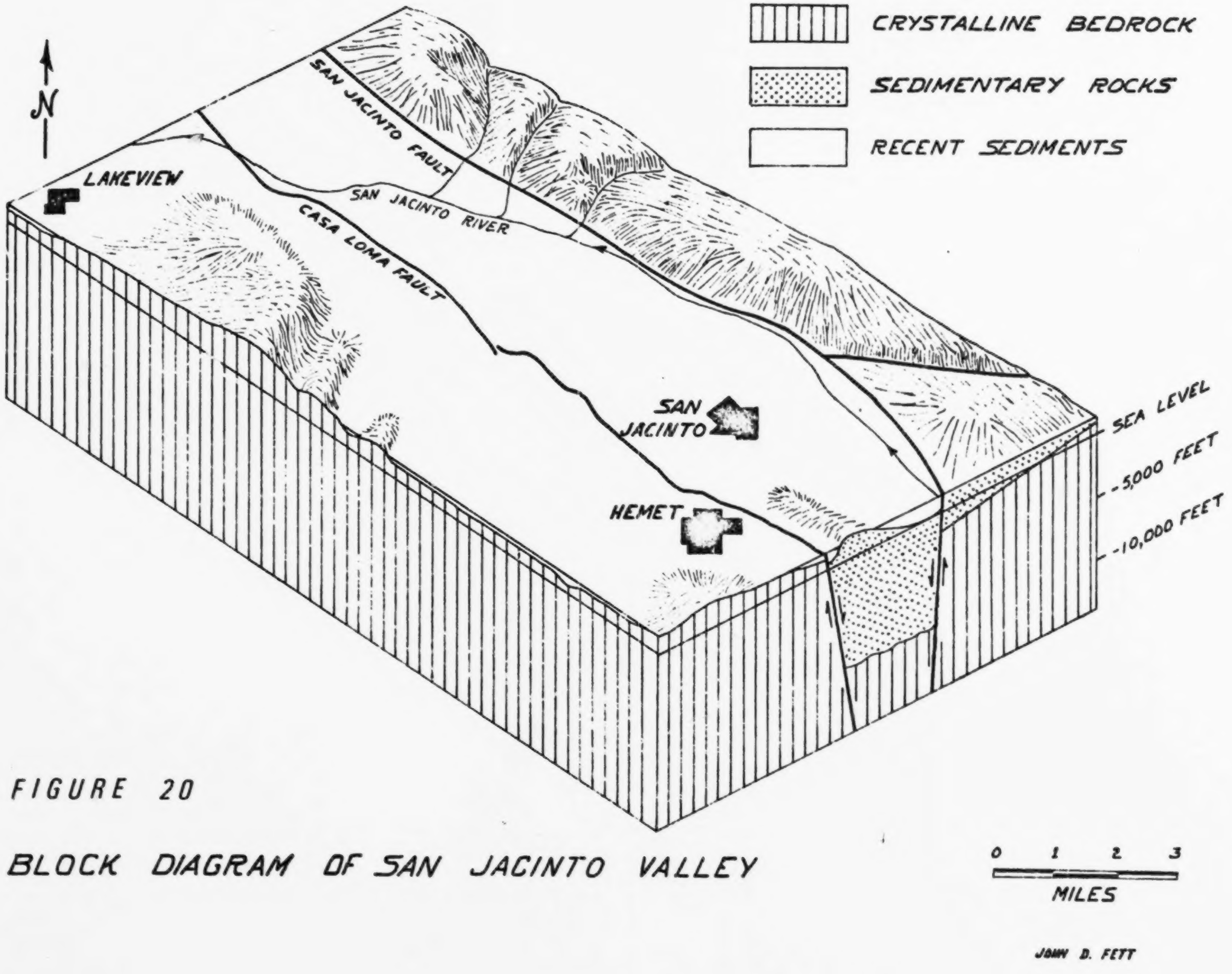
CRYSTALLINE BEDROCK
SEDIMENTARY ROCKS
RECENT SEDIMENTS
N
LAKEVIEW
SAN JACINTO FAULT
SAN JACINTO RIVER
CASA LOMA FAULT
SAN JACINTO
HEMET
SEA LEVEL
-5,000 FEET
-10,000 FEET
0
1
2
3
MILES
JOHN D. FETT

FIGURE 20

BLOCK DIAGRAM OF SAN JACINTO VALLEY

ACKNOWLEDGEMENT

Dr. Gordon P. Eaton, of the University of California at Riverside, suggested the gravity survey in the San Jacinto valley because of the writer's familiarity with its geology. Dr. Eaton later arranged with Eastern Municipal Water District to have the District pay for explosives for the seismic work, and supply the men and equipment for placing the charges. (Dr. Eaton also arranged to have the District do leveling so he and his students could extend the gravity work of the writer.)

Drs. Shawn Biehler and Stewart Smith, of the California Institute of Technology, together with some of their students, recorded about half the data from Shot Point 1 and supervised shotpoint operations at Shot Point 1.

Dr. Eaton and the writer, with the aid of UCR graduate students, recorded the data of Line A from Shot Point 2.

Eastern Municipal Water District, and in particular James Linehan of the District, made the seismic work possible. Without their financial support for explosives and their men and equipment for planting the explosives, the project would not have been possible. They also supplied radio equipment for transmitting shot time information and coordinating spread and shotpoint work.

REFERENCES

Allen, C. R., P. St. Amand, C. F. Richter, and J. M. Nordquist, 1965, Relationship between seismicity and geologic structure in southern California: Bull. Seismological Soc. Amer., vol. 55, no. 4, pp. 753-798.

Bean, Robert T., 1955, Geology of San Jacinto and Elsinore basins: State Water Resources Board, Santa Ana River Investigation, Bull. 15, Appendix B, 88 p.

Dudley, P. H., 1936, Physiographic history of a portion of the Perris Block, southern California: Jour. Geol., vol. 44, pp. 358-378.

English, W. A., 1926, Geology and oil resources of the Puente Hills region, southern California: U. S. Geological Survey Bull. 768, 110 p.

Fett, J. D., D. H. Hamilton, and F. A. Fleming, 1967, Continuing surface displacements along the Casa Loma and San Jacinto faults in San Jacinto valley, Riverside County, California: Engineering Geology, vol. 4, no. 1, pp. 22-32.

Fett, J. D., and D. H. Hamilton, 1968, Subsidence and "fault creep" in the San Jacinto valley, Riverside County, California: in preparation, to be submitted to Engineering Geology.

Fraser, D. M., 1931, Geology of San Jacinto quadrangle south of San Gorgonio Pass, California: Mining in California (Calif. Jour. of Mining and Geology), vol. 27, pp. 494-540.

Frick, Childs, 1921, Extinct vertebrate faunus of the Badlands of Bautista creek and San Timoteo canyon, southern California: Univ. Calif. Pub., Bull. Dept. Geol. Sci., vol. 12, no. 5, pp. 277-424.

Gibbs, H. J., and J. P. Bara, 1967, Stability problems of collapsing soil: Jour. Soil Mech. and Found. Div., Proc. Amer. Soc. Civil Eng., vol. 93, SM4, pp. 577-594.

Green, R., 1962, The hidden layer problem: Geophysical Prospecting, vol. 10, pp. 166-170.

Mann, J. F., 1955, Geology of a portion of the Elsinore fault zone, California: Calif. Div. of Mines, Special Report 43, 22 p.

McCulloh, T. H., 1967, Mass properties of sedimentary rocks and gravimetric effects of petroleum and natural-gas reservoirs: U. S. Geological Survey Prof. Paper 528-A, 50 p.

O'Brien, P. N. S., 1967, The efficient use of large charges: in SEISMIC REFRACTION PROSPECTING, A. W. Musgrave, editor, Society of Exploration Geophysicists, Tulsa, Oklahoma, pp. 152-170.

Proctor, R. J., 1962, Geologic features of a section across the Casa Loma fault, exposed in an aqueduct trench near San Jacinto, California: Geol. Soc. Amer. Bull., vol. 73, pp. 1293-1296.

Sharp, R. V., 1967, San Jacinto fault zone in the Peninsular

Ranges of southern California: Geol. Soc. Amer. Bull., vol. 78, no. 6, pp. 705-730.

Townley, Sidney D., 1918, The San Jacinto earthquake of April 21, 1918: Bull. Seismological Soc. Amer., vol. 8, no. 2, pp. 44-62.

Waring, G. A., 1919, Ground water in the San Jacinto and Temecula basins, California: U. S. Geological Survey Water Supply Paper 429, 113 p.

APPENDIX: GRAVITY DATA

Column 1: Station number

Column 2: Latitude in degrees, minutes, and hundredths of a minute (example: 334403 is 33° 44.03')

Column 3: Longitude

Column 4: Elevation in tenths of a foot if followed by a T and in feet if followed by a U (example: 17360T is 1736.0 feet above sea level; 1717U is 1717 feet above sea level)

Column 5: Observed gravity minus 978,000.00 milligals (example: 143737 is 979,437.37 milligals)

Column 6: Theoretical gravity at sea level minus 978,000.00 milligals (example: 163921 is 979,639.21 milligals)

Column 7: Free air anomaly in hundredths of a milligal (example: -3855 is -38.55 milligals)

Column 8: Bouguer anomaly in hundredths of a milligal plus 1,000.00 milligals (example: 90318 is 1,000.00 - 903.18 = -96.82 milligals) 2.67 rock density used for correction

Column 9: Bouguer anomaly, as above, but with 2.00 rock density used for correction.

	1	2	3	4	5	6	7	8	9
JF	101	334403	1165564	17360T	143737	163921	-3855	90318	91780
JF	102	334410	1165564	17275T	143609	163930	-4072	90133	91588
JF	103	334422	1165564	17218T	143414	163947	-4338	89886	91335
JF	104	334433	1165564	1717U	143247	163962	-4566	89674	91120
JF	105	334444	1165564	1711U	143106	163978	-4778	89482	90922
JF	106	334453	1165564	1708U	142950	163990	-4975	89295	90733
JF	107	334465	1165564	17041T	142810	164007	-5168	89117	90551
JF	108	334476	1165564	1701U	142678	164022	-5344	88951	90383
JF	109	334487	1165564	1699U	142570	164037	-5486	88815	90245
JF	110	334497	1165564	1696U	142464	164051	-5625	88677	90105
JF	111	334508	1165564	16934T	142559	164066	-5580	88741	90166
JF	112	334508	1165537	16980T	142268	164066	-5827	88478	89907
JF	113	334487	1165537	17070T	142330	164037	-5651	88623	90060
JF	114	334476	1165537	17110T	142397	164022	-5532	88728	90169
JF	115	334465	1165537	17150T	142513	164007	-5362	88885	90328
JF	116	334455	1165537	17210T	142637	163993	-5168	89056	90506
JF	117	334444	1165537	1724U	142808	163978	-4954	89261	90712
JF	118	334434	1165537	1727U	142973	163964	-4746	89459	90913
JF	119	334422	1165537	17275T	143163	163947	-4525	89670	91124
JF	120	334412	1165537	1738U	143298	163933	-4287	89881	91345
JF	121	334400	1165537	17425T	143520	163916	-4006	90146	91613
JF	122	334381	1165512	1765U	143475	163890	-3814	90272	91756
JF	123	334390	1165512	1760U	143305	163903	-4043	90058	91539
JF	124	334400	1165512	1757U	143152	163916	-4238	89871	91349
JF	125	334409	1165512	17521T	143011	163929	-4438	89690	91164
JF	126	334422	1165512	17463T	142854	163947	-4667	89470	90948
JF	127	334444	1165512	1735U	142531	163978	-5127	89057	90516
JF	128	334465	1165512	17208T	142280	164007	-5541	88694	90141
JF	129	334487	1165512	17138T	142088	164037	-5829	88430	89871
JF	130	334530	1165512	16935T	141867	164097	-6300	88034	89456
JF	131	334552	1165512	1679U	141850	164127	-6476	87910	89319
JF	132	334577	1165513	1664U	141913	164162	-6608	87851	89244
JF	133	334575	1165485	1671U	141830	164159	-6612	87825	89221
JF	134	334552	1165485	16685T	141754	164127	-6492	87873	89287
JF	135	334531	1165484	17010T	141733	164098	-6366	87954	89380
JF	136	334506	1165484	1716U	141750	164066	-6176	88086	89526
JF	137	334487	1165484	17260T	141832	164037	-5971	88256	89705
JF	138	334497	1165456	1738U	141649	164037	-6041	88144	89603
JF	139	334487	1165427	1745U	141557	164037	-6067	88117	89576
JF	140	334487	1165305	1757U	141485	164037	-6026	88115	89585
JF	141	334510	1165427	1727U	141579	164069	-6246	88001	89445
JF	143	334466	1165484	1735U	141995	164008	-5694	88502	89959
JF	144	334444	1165484	1747U	142259	163978	-5286	88666	90333
JF	145	334422	1165494	1762U	142544	163947	-4830	89272	90752
JF	146	334466	1165457	1748U	141746	164008	-5820	88331	89708
JF	147	334466	1165427	1761U	141591	164008	-5853	88274	89748
JF	148	334444	1165414	1778U	141608	163978	-5646	88420	89909
JF	149	334444	1165459	1761U	141939	163978	-5476	88625	90107
JF	150	334422	1165459	17805T	142243	163947	-4957	89080	90576

NOT REPRODUCIBLE

	1	2	3	4	5	6	7	8	9
JF	151	334422	1165381	1812U	141440	163947	-5463	88510	90022
JF	152	334378	1165381	1843U	141790	163886	-4761	89104	90643
JF	153	334378	1165398	1836U	142025	163886	-4591	89274	90814
JF	154	334378	1165459	18021T	142763	163886	-4173	89793	91307
JF	155	334378	1165484	1782U	143130	163886	-3985	90053	91549
JF	156	334422	1165616	1695U	143959	163947	-4045	90256	91686
JF	157	334422	1165642	1677U	144209	163947	-3964	90393	91809
JF	158	334422	1165668	16672T	144434	163947	-3831	90553	91962
JF	159	334421	1165694	16526T	144650	163946	-3751	90683	92080
JF	160	334421	1165720	16402T	144827	163946	-3691	90774	92163
JF	161	334421	1165747	1628U	144[illegible]74	163946	-3659	90849	92227
JF	162	334421	1165772	16185T	145128	163946	-3593	90940	92312
JF	163	334421	1165799	1606U	145259	163946	-3581	909[illegible]2	92354
JF	164	334420	1165825	15943T	145403	163944	-3545	91067	92419
JF	165	334420	1165851	1582U	145575	163944	-3469	91157	92500
JF	166	334420	1165877	1570U	145772	163944	-3405	91283	92616
JF	167	334420	1165903	1558U	145916	163944	-3373	91352	92676
JF	168	334442	1165877	1571U	145754	163975	-3444	91241	92574
JF	169	334442	1165929	1552U	146022	163975	-3355	91386	92707
JF	170	334442	1165851	1584U	145538	163975	-3538	91101	92446
JF	171	334442	1165825	1595U	145380	163975	-3592	91017	92370
JF	172	334442	1165799	1606U	145217	163975	-3652	90920	92282
JF	173	334442	1165772	1619U	145036	163975	-3691	90841	92213
JF	174	334442	1165747	1628U	144920	163975	-3742	90765	92143
JF	175	334443	1165720	1642U	144836	163976	-3695	90762	92153
JF	389	334787	1165570	1616U	143220	164454	-6014	88784	90090
JF	177	334443	1165694	1654U	144652	163976	-3767	90661	92059
JF	178	334443	1165668	1667U	144501	163976	-3996	90387	91797
JF	179	334443	1165642	1676U	144021	163976	-4191	90167	91583
JF	180	334444	1165616	1692U	143712	163976	-4351	89959	91387
JF	181	334465	1165616	16[illegible]T	143460	164007	-4663	89646	91069
JF	182	334465	1165642	1675U	143784	164007	-4467	89894	91309
JF	183	334465	1165668	16[illegible]T	14413[illegible]	164007	-4226	90168	91575
JF	184	334464	1165694	1652U	1444[illegible]	164005	-398[illegible]	90446	9184[illegible]
JF	185	334464	1165720	16426T	144828	164005	-3727	90728	92114
JF	186	334464	1165747	16275T	144949	164005	-3748	90759	92138
JF	187	334464	1165772	16197T	145022	164005	-3748	90780	92153
JF	188	334464	1165799	1605U	145119	164005	-3790	90785	92147
JF	189	334464	1165825	15947T	145269	164005	-3737	90873	92226
JF	190	334463	1165851	1582U	145447	164004	-3676	90960	92313
JF	191	334463	1165877	15752T	145631	164004	-3556	91113	92451
JF	192	334463	1165902	1562U	145813	164004	-3409	91213	92540
JF	193	334463	1165929	1556U	145921	164004	-3448	91281	92604
JF	194	334485	1165929	1556U	145804	164034	-3595	91134	92457
JF	195	334485	1165902	1568U	145629	164034	-3657	91034	92366
JF	196	334485	1165877	15755T	145469	164034	-3746	90922	92260
JF	197	334485	1165851	1586U	145306	164034	-3810	90821	92169
JF	198	334486	1165825	1592U	145176	164036	-3886	90734	92084
JF	199	334486	1165799	1600U	145041	164036	-3945	90647	92004

```
     1      2         3       4        5       6       7      8      9
JF 200 334486 1165772 1611U   144963 164036 -3919 90639 92004
JF 201 334486 1165747 1625U   144866 164036 -3886 90630 92007
JF 202 334487 1165720 1636U   144678 164037 -3971 90507 91893
JF 203 334487 1165694 1646U   144256 164037 -4298 90157 91548
JF 204 334487 1165668 1657U   143850 164037 -4601 89816 91217
JF 205 334487 1165642 1664U   143584 164037 -4801 89598 91003
JF 206 334487 116561616795T   143215 164037 -5025 89329 90746
JF 207 334399 1165616 1696U   144163 163915 -3800 90499 91930
JF 208 334399 116564216836T   144335 163915 -3744 90591 92013
JF 209 334399 1165668 1667U   144544 163915 -3692 90695 92104
JF 210 334399 1165694 1652U   144728 163915 -3649 90789 92185
JF 211 334399 1165720 1640U   144896 163915 -3593 90875 92263
JF 212 334399 1165747 1626U   145060 163915 -3561 90956 92332
JF 213 334398 1165772 1613U   145185 163914 -3557 90998 92365
JF 214 334377 116577216165T   145322 163885 -3358 91188 92556
JF 215 334377 1165747 1631U   145168 163885 -3375 91128 92507
JF 216 334378 116561616903T   144344 163886 -3643 90681 92106
JF 217 334378 1165642 1678U   144515 163886 -3587 90772 92188
JF 218 334378 116566816704T   144660 163886 -3514 90866 92276
JF 219 334377 1165694 1658U   144794 163885 -3495 90926 92326
JF 220 334377 116572016464T   144969 163885 -3430 91020 92413
JF 221 334377 1165799 1601U   145458 163885 -3368 91226 92583
JF 222 334377 116582515897T   145567 163885 -3365 91267 92614
JF 223 334377 1165851 1578U   145688 163885 -3354 91308 92648
JF 224 334398 1165851 1582U   145591 163914 -3442 91205 92548
JF 225 334398 1165825 1594U   145439 163914 -3482 91133 92484
JF 226 334398 1165799 1603U   145306 163914 -3530 91055 92414
JF 227 334355 116579816045T   145588 163854 -3174 91409 92768
JF 228 334355 116582515885T   145788 163854 -3125 91512 92858
JF 229 334305 1165825 1584U   146034 163785 -2851 91805 93146
JF 230 334377 116587715672T   145816 163885 -3327 91372 92702
JF 231 334398 1165877 1573U   145759 163914 -3359 91318 92654
JF 232 334398 1165900 1560U   145895 163914 -3345 91374 92699
JF 233 334376 1165929 1550U   146110 163883 -3194 91556 92874
JF 234 334356 116561616995T   144418 163855 -3452 90847 92278
JF 235 334338 116561617149T   144415 163830 -3285 90963 92407
JF 236 334356 1165642 1689U   144617 163855 -3351 90974 92398
JF 237 334359 1165668 1684U   144774 163860 -3246 91089 92510
JF 238 334506 116592915586T   145692 164064 -3711 91008 92334
JF 239 334507 1165903 1563U   145517 164065 -3847 90861 92189
JF 240 334507 116587615718T   145387 164065 -3893 90787 92122
JF 241 334507 1165851 1579U   145240 164065 -3973 90683 92024
JF 242 334507 116582415878T   145080 164065 -4050 90584 91930
JF 243 334507 1165798 1594U   144917 164065 -4155 90458 91810
JF 244 334507 116577216083T   144809 164065 -4129 90439 91802
JF 245 334507 1165746 1620U   144682 164065 -4145 90388 91760
JF 246 334508 116572116297T   144421 164066 -4317 90182 91563
JF 247 334508 1165694 1634U   144036 164066 -4661 89835 91216
JF 248 334508 116566816553T   143615 164066 -4882 89540 90940
```

	1	2	3	4	5	6	7	8	9
JF	249	334508	1165642	1687U	143159	164066	-5039	89280	90705
JF	250	334502	1165615	16834T	143040	164058	-5184	89155	90576
JF	251	334529	1165671	1682U	143183	164095	-5091	89241	90664
JF	252	334529	1165694	1634U	143726	164095	-5000	89500	90880
JF	253	334529	1165721	1620U	144118	164095	-4740	89795	91166
JF	254	334529	1165747	1615U	144423	164095	-4482	90071	91438
JF	255	334529	1165773	1604U	144628	164095	-4380	90204	91563
JF	256	334528	1165799	15916T	144800	164094	-4323	90300	91649
JF	257	334528	1165825	1583U	144989	164094	-4216	90437	91779
JF	258	334528	1165851	1574U	145182	164094	-4107	90568	91904
JF	259	334528	1165877	1567U	145350	164094	-4004	90695	92025
JF	260	334550	1165930	1549U	145684	164125	-3871	90883	92200
JF	261	334550	1165878	15646T	145337	164125	-4071	90636	91964
JF	262	334550	1165851	1573U	145116	164125	-4213	90465	91801
JF	263	334550	1165825	1580U	144885	164125	-4378	90286	91625
JF	264	334551	1165773	15969T	144640	164126	-4465	90144	91497
JF	265	334551	1165799	1590U	144426	164126	-4745	89884	91232
JF	266	334551	1165747	1605U	144149	164126	-4880	89707	91066
JF	267	334551	1165722	16107T	143809	164126	-5166	89401	90764
JF	268	334400	1165484	1776U	142816	163916	-4395	89658	91150
JF	269	334400	1165459	1792U	142505	163916	-4556	89440	90947
JF	270	334530	1165559	1682U	142367	164097	-5909	88456	89870
JF	271	334530	1165537	1686U	142107	164097	-6131	88220	89638
JF	272	334552	1165537	16755T	141987	164127	-6330	88008	89416
JF	273	334574	1165538	1662U	141960	164158	-6565	87880	89274
JF	274	334592	1165538	1652U	141985	164183	-6659	87822	89207
JF	275	334592	1165563	1648U	142060	164183	-6622	87873	89254
JF	276	334574	1165563	1658U	142066	164158	-6497	87962	89353
JF	277	334616	1165565	1626U	142149	164216	-6773	87801	89163
JF	278	334616	1165611	1620U	142262	164216	-6717	87857	89219
JF	279	334615	1165701	1587U	142831	164215	-6456	88215	89552
JF	280	334615	1165721	1580U	142995	164215	-6358	88322	89657
JF	281	334615	1165748	1572U	143259	164215	-6169	88530	89867
JF	282	334564	1165747	1578U	143797	164172	-5532	89155	90488
JF	283	334592	1165701	1601U	143074	164183	-6050	88572	89921
JF	284	334592	1165583	1643U	142151	164183	-6537	87915	89297
JF	285	334552	1165698	1638U	143410	164127	-5311	89175	90559
JF	286	334637	1165743	1563U	143061	164245	-6482	88267	89584
JF	287	334637	1165774	1553U	143324	164245	-6313	88462	89773
JF	288	334637	1165826	15373T	144016	164245	-5770	89054	90352
JF	289	334636	1165878	15467T	144734	164244	-4962	89817	91127
JF	290	334636	1165905	15485T	145113	164244	-4566	90201	91514
JF	291	334636	1165931	15354T	145488	164244	-4314	90494	91797
JF	292	334636	1165957	15315T	145812	164244	-4026	90795	92094
JF	293	334636	1165983	15279T	146086	164244	-3787	91040	92338
JF	294	334615	1165983	1527U	146105	164215	-3747	91080	92378
JF	295	334594	1165983	15295T	146122	164186	-3678	91141	92441
JF	296	334572	1165983	1534U	146124	164155	-3603	91200	92504
JF	297	334549	1165983	15373T	146098	164123	-3565	91224	92532

	1	2	3	4	5	6	7	8	9
JF	298	334464	1165982	1539U	146116	164033	-3441	91341	92651
JF	299	334506	1165983	15412T	146083	164064	-3484	91290	92601
JF	300	334526	1165983	1537U	146084	164091	-3551	91239	92547
JF	301	334572	1165955	1537U	145894	164155	-3804	90994	92300
JF	302	334572	1165930	15445T	145662	164155	-3966	90807	92118
JF	303	334572	1165903	1552U	145490	164155	-4067	90683	92001
JF	304	334572	1165876	15590T	145324	164155	-4167	90563	91886
JF	305	334550	1165903	1556U	145531	164125	-3957	90776	92097
JF	306	334550	1165955	1545U	145870	164125	-3722	91046	92359
JF	307	334594	1165957	1536U	145860	164186	-3878	90923	92228
JF	308	334594	1165930	15414T	145611	164186	-4076	90707	92016
JF	309	334594	1165903	1548U	145393	164186	-4233	90531	91845
JF	310	334594	1165876	15562T	145233	164186	-4315	90425	91744
JF	311	334500	1165590	16890T	142793	164055	-5375	88944	90369
JF	312	334487	1165570	1690U	142886	164037	-5255	89061	90487
JF	313	334465	1165590	1693U	143161	164007	-4921	89385	90814
JF	314	334444	1165590	1705U	143306	163978	-4544	89720	91159
JF	315	334422	1165590	1710U	143684	163947	-4179	90070	91513
JF	316	334399	1165590	1710U	144009	163915	-3822	90429	91871
JF	317	334377	1165590	1704U	144190	163885	-3667	90611	92047
JF	318	334356	1165589	1714U	144213	163855	-3520	90729	92172
JF	319	334338	1165589	1725U	144246	163830	-3359	90856	92308
JF	320	334528	1165930	1554U	145668	164094	-3809	90928	92249
JF	321	334614	1165930	1539U	145555	164213	-4183	90608	91915
JF	322	334659	1165931	1533U	145361	164276	-4496	90321	91621
JF	323	334680	1165983	15238T	145974	164305	-3998	90847	92141
JF	324	334680	1165957	1527U	145597	164305	-4345	90497	91791
JF	325	334681	1165932	15308T	145102	164306	-4806	90024	91321
JF	326	334681	1165905	1521U	144702	164306	-5297	89571	90859
JF	327	334681	1165866	15240T	144012	164306	-5959	88906	90194
JF	328	334682	1165826	15312T	143497	164308	-6408	88445	89737
JF	329	334682	1165800	1541U	143203	164308	-6610	88210	89510
JF	330	334682	1165774	15485T	142963	164308	-6780	88021	89326
JF	331	334682	1165748	1557U	142794	164308	-6868	87913	89223
JF	332	334652	1165702	15755T	142643	164266	-6804	87919	89243
JF	333	334652	1165661	1594U	142407	164266	-6866	87793	89134
JF	334	334552	1165607	16100T	142236	164127	-6748	87852	89207
JF	335	334116	1165725	1679U	145395	163523	-2335	92029	93444
JF	336	334323	1165595	17174T	144446	163810	-3210	91041	92483
JF	337	334321	1165563	1724U	144280	163807	-3311	90937	92380
JF	338	334336	1165459	1852U	143037	163828	-3371	90432	91987
JF	339	334357	1165505	1801U	143502	163857	-3414	90562	92074
JF	340	334529	117 213	15072T	147890	164095	-2029	92861	94143
JF	341	335026	117 397	1491U	147839	164786	-2922	92055	93315
JF	342	334702	1165932	1518U	144864	164336	-5193	89681	90967
JF	343	334724	1165932	15141T	144569	164366	-5556	89332	90615
JF	344	334745	1165932	15053T	144331	164395	-5906	89020	90293
JF	345	334768	1165932	15001T	144097	164427	-6221	88725	89993
JF	346	334824	1165932	1495U	143693	164505	-6750	88225	89486

	1	2	3	4	5	6	7	8	9
JF	347	334848	1165926	14895T	143569	164538	-6959	88049	89302
JF	348	334863	1165906	14890T	143435	164559	-7119	87906	89155
JF	349	334697	1165906	1486U	143474	164606	-7155	87904	89144
JF	350	335003	1165920	1496U	144513	164754	-6169	88923	90155
JF	351	334525	117 697	1722U	147962	164090	70	94236	95700
JF	352	334635	117 538	2219U	145455	164243	2084	94572	96457
JF	353	334802	117 538	1760U	147910	164474	-10	94031	95527
JF	354	334436	1165720	16385T	144834	163966	-3721	90750	92137
JF	355	334385	1165720	1642U	144940	163896	-3511	90953	92342
JF	356	334376	1165881	1568U	145835	163883	-3299	91397	92728
JF	357	334376	1165929	1550U	146112	163883	-3192	91558	92876
JF	358	334285	1165929	1562U	146680	163757	-2385	92327	93654
JF	359	334332	1165928	1546U	146467	163822	-2814	91952	93265
JF	360	334398	1165929	1549U	146056	163914	-3287	91466	92782
JF	361	334419	1165929	1550U	146039	163943	-3324	91426	92743
JF	362	334376	117 35	15259T	146799	163883	-2732	92092	93391
JF	363	334409	117 29	1520U	146730	163929	-2902	91942	93236
JF	364	334463	117 35	15220T	146645	164004	-3043	91795	93091
JF	365	334484	117 35	1524U	146584	164033	-3114	91717	93014
JF	366	334506	117 35	1524U	146556	164064	-3173	91658	92955
JF	367	334506	117 5	1532U	146329	164064	-3325	91481	92785
JF	368	334506	1165954	1549U	145856	164064	-3637	91115	92432
JF	369	334572	1165825	1577U	144718	164155	-4604	90074	91410
JF	370	334592	1165825	15635T	144593	164183	-4884	89841	91165
JF	371	334620	1165826	15410T	144264	164222	-5463	89342	90646
JF	372	334637	1165801	15415T	143648	164245	-6098	88711	90014
JF	373	334605	1165773	15595T	143747	164201	-5785	88960	90278
JF	374	334547	1165574	1669U	142295	164120	-6127	88284	89686
JF	375	334561	1165596	1653U	142390	164140	-6201	88247	89640
JF	376	334579	1165639	16295T	142655	164165	-6182	88356	89727
JF	377	334592	1165672	1615U	142783	164183	-6210	88363	89725
JF	378	334592	1165648	1618U	142662	164183	-6302	88260	89624
JF	379	334592	1165625	1627U	142443	164183	-6436	88111	89459
JF	380	334616	1165592	1625U	142173	164216	-6759	87707	89163
JF	381	334616	1165635	16115T	142394	164216	-6664	87939	89204
JF	382	334633	1165701	1583U	142716	164240	-6635	88061	89302
JF	383	334634	1165659	1595U	142459	164241	-6780	87874	89216
JF	384	334634	1165635	1603U	142342	164241	-6821	87824	89168
JF	385	334682	1165604	1604U	142279	164308	-6942	87722	89061
JF	386	334703	1165626	1594U	142335	164337	-7009	87696	89025
JF	387	334724	1165583	1596U	142566	164366	-6788	87930	89262
JF	388	334744	1165557	1632U	142750	164394	-6233	88366	89706
JF	390	334861	1165664	-0	143155	164556	-21401	80825	80266
JF	391	334897	1165752	-0	143791	164606	-20815	81246	80729
JF	392	334897	1165828	15035T	143401	164606	-7063	88050	89276
JF	393	334866	1165828	15125T	143148	164563	-7189	87834	89083
JF	394	334816	1165828	1519U	143011	164494	-7195	87746	89015
JF	395	334787	1165849	1521U	143137	164454	-7010	87890	89170
JF	396	334772	1165868	1520U	143319	164433	-6817	88078	89359

1	2	3	4	5	6	7	8	9
JF 397	334724	1165826	1532U	143196	164366	-6760	88095	89386
JF 398	334583	1165773	15665T.	144145	164170	-5291	89429	90754
JF 399	334575	1165722	1631U	143343	164159	-5475	89027	90407
JF 400	334574	1165705	1614U	143290	164158	-5687	88881	90244
JF 401	334572	117 35	1521U	146490	164155	-3359	91486	92780.
JF 402	334637	117 35	1517U	146602	164245	-3374	91488	92777
JF 403	334682	117 35	1515U	146497	164308	-3561	91311	92598
JF 404	334723	117 36	1510U	146313	164365	-3849	91038	92321
JF 405	334798	117 36	1496U	145410	164469	-4987	89957	91226
JF 406	334762	117 36	1502U	145866	164419	-4425	90493	91768
JF 407	334723	1165984	15161T	145470	164365	-4634	90238	91525
JF 408	334723	1165957	1513U	145053	164365	-5081	89811	91093
JF 409	334747	1165801	15365T	142912	164398	-7034	87819	89110
JF 410	334762	1165783	1539U	142789	164419	-7154	87699	88990
JF 411	334725	1165748	1556U	142646	164368	-7086	87709	89015
JF 412	334791	1165749	1543U	142744	164459	-7202	87685	88968
JF 413	334811	1165749	1540U	142816	164487	-7186	87741	89014
JF 414	334811	1165723	1548U	142822	164487	-7105	87816	89091
JF 415	334827	1165703	1543U	143022	164509	-6973	88043	89293
JF 416	334805	1165678	1547U	142905	164479	-7023	87963	89221
JF 417	334757	1165723	1557U	142592	164412	-7175	87644	88944
JF 418	334749	1165670	15745T	142531	164401	-7060	87724	89033
JF 419	334726	1165670	15815T	142461	164369	-7033	87704	89025
JF 420	334703	1165670	15815T	142392	164337	-7069	87655	88979
JF 421	334682	1165669	1587U	142383	164308	-6998	87700	89031
JF 422	334682	1165702	15745T	142527	164308	-6971	87768	89088
JF 423	334666	1165702	1574U	142459	164286	-7022	87708	89031
JF 425	334667	1165637	1597U	142311	164287	-6954	87718	89055
JF 426	334780	117 217	15093T	147554	164444	-2693	92228	93502
JF 424	334305	1165825	1587U	142414	163785	-6443	88203	89546

SEISMIC DATA - LINE A

Spread	Distance*	Time
UCR-I	74 feet	0.057
	260	0.092
	469	0.133
	678	0.177
	883	0.208
	1094	0.247
	1392	0.284
	1553	0.320
	1763	0.358
	1970	0.394
	2176	0.429
	2384	0.468
UCR-II	9,000	1.522
	9,200	1.556
	9,400	1.589
	9,600	1.623
	9,800	1.652
	10,000	1.674
	10,233	1.710
	10,438	1.731
	10,641	1.764
	10,843	1.794
	11,049	1.820
	11,250	1.841
JDF-I	11,250	1.841
	11,349	1.862
	11,448	1.873
	11,547	1.887
	11,646	1.906
	11,745	1.919
	11,844	1.929
	11,943	1.943
	12,042	1.959
	12,141	1.976
	12,240	1.991
	12,340	2.006

Spread	Distance	Time
CIT-I	13,700	2.184
	13,900	2.212
	14,100	2.238
	14,300	2.266
	14,500	2.293
	14,700	2.313
	14,900	2.342
	15,100	2.372
CIT-II	15,300	2.408
	15,500	2.429
	15,700	2.451
	15,900	2.471
	16,100	2.502
	16,300	2.520
	16,500	2.544
	16,700	2.562
CIT-III	18,100	2.731
	18,300	2.761
	18,500	2.776
	18,700	2.797
	18,900	2.808
	19,100	2.838
	19,300	2.864
	19,500	2.883
JDF-II	18,785	2.793
	18,885	2.809
	18,985	2.823
	19,085	2.836
	19,185	2.853
	19,285	2.861
	19,385	2.871
	19,485	2.871
	19,585	2.885
	19,685	2.903
	19,785	
	19,885	2.925

* Distance from Shot Point 1 at northwest end of line

Line A continued

Spread	Distance	Time	
CIT-IV	19,900	2.947	
	20,100	2.967	
	20,300	3.001	
	20,500	3.035	
	20,700	3.052	
	20,900	3.067	
	21,100	3.089	
CIT-V	28,900	3.789	
	29,100	3.809	
	29,300	3.823	
	29,500	3.842	
	29,700	3.862	
	29,900	3.875	
	30,100	3.897	
	30,300	3.911	
CIT-VI	31,100	4.038	
	31,300	4.044	
	31,500	4.076	
	31,700	4.106	
	31,900	4.139	
	32,100	4.154	
	32,300	4.176	
	32,500	4,188	
JDF-III	34,800	4.348	4.429
	34,900	4.354	4.438
	35,000	4.357	4.441
	35,100	4.360	4.447
	35,200	4.371	4.454
	35,300	4.380	4.456
	35,400	4.379	4.462
	35,500	4.383	4.467
	35,600		
	35,700		
	35,800	4.390	
	35,900		

Line A continued

Spread	Distance*	Time	Spread	Distance	Time
1	1,300	0.470	4	7,936	1.451
	1,490	0.492		8,125	1.478
	1,680	0.515		8,314	1.509
	1,870	0.535		8,503	1.530
	2,060	0.552		8,692	1.557
	2,250	0.580		8,881	1.588
	2,450	0.615		9,070	1.624
	2,620	0.645		9,259	1.655
	2,810	0.673		9,448	1.679
	3,000	0.706		9,637	1.715
	3,200	0.732		9,826	1.734
	3,400	0.760		10,015	1.756
2	3,400	0.760	5	10,204	1.777
	3,589	0.785		10,393	1.796
	3,778	0.812		10,582	1.816
	3,967	0.849		10,761	1.838
	4,156	0.875		10,950	1.868
	4,345	0.903		11,139	1.907
	4,534	0.929		11,328	1.931
	4,723	0.954		11,517	1.960
	4,912	0.987		11,706	1.978
	5,101	1.008		11,895	2.004
	5,290	1.038		12,084	2.033
	5,479	1.066		12,273	2.047
3	5,668	1.094	6	14,100	2.223
	5,857	1.116		14,291	2.249
	6,046	1.144		14,481	2.271
	6,235	1.179		14,672	2.294
	6,424			14,863	2.315
	6,613	1.235		15,054	
	6,802	1.267		15,245	2.359
	6,991	1.294		15,436	2.377
	7,180	1.329		15,621	2.403
	7,369	1.364		15,812	2.427
	7,558	1.388		16,003	2.443
	7,747	1.420		16,194	2.471

Distance between Shot Points 1 and 2: 39,430 feet

* Distance from Shot Point 2 at southeast end of line

Line A continued

Spread	Distance*	Time	Spread	Distance	Time
7	18,400	2.787	10	26,300	3.637
	18,600	2.817		26,500	3.648
	18,800	2.835		26,700	3.659
	19,000	2.861		26,900	3.671
	19,200	2.867		27,100	3.685
	19,400	2.893		27,300	
	19,600	2.925		27,500	3.707
	19,800	2.952		27,700	3.719
	20,000	2.965		27,900	3.731
	20,200	2.986		28,100	3.743
	20,400	3.007		28,300	3.758
	20,600	3.031		28,500	3.769
8	20,800	3.035	11	28,700	3.780
	21,000	3.060		28,900	3.788
	21,200	3.075		29,100	3.799
	21,400	3.095		29,300	3.809
	21,600	3.115		29,500	3.819
	21,800	3.137		29,700	
	22,000	3.185		29,900	3.839
	22,200	3.198		30,100	3.849
	22,400	3.210		30,300	3.859
	22,600	3.225		30,500	3.869
	22,800	3.240		30,700	3.879
	23,000	3.255		30,900	3.889
9	23,900	3.516**			
	24,100	3.523			
	24,300	3.533			
	24,500	3.543			
	24,700	3.553			
	24,900				
	25,100	3.573			
	25,300	3.584			
	25,500	3.595			
	25,700	3.605			
	25,900	3.616			
	26,100	3.626			

* Distance from Shot Point 2

** This and following travel-times are not first breaks

SEISMIC DATA - LINE B

Spread	Distance*	Time	Spread	Distance	Time
1	50	0.067	4	5,230	1.022
	100	0.099		5,409	1.047
	200	0.152		5,588	1.077
	300	0.207		5,767	1.107
	400	0.252		5,948	1.137
	500			6,125	1.162
	600	0.334		6,304	
	700	0.358		6,483	1.208
	800	0.372		6,662	1.231
	900	0.393		6,841	1.260
	1,000	0.405		7,020	1.288
	1,100	0.423		7,199	1.306
2	1,300	0.452	5	10,600	1.758
	1,395	0.469		10,800	1.778
	1,492	0.486		11,000	1.811
	1,593	0.497		11,200	1.828
	1,691	0.516		11,400	1.852
	1,791	0.528		11,600	1.883
	1,890			11,800	
	1,990	0.558		12,000	1.913
	2,090	0.573		12,200	1.928
	2,190	0.587		12,400	1.933
	2,290	0.597		12,600	1.947
	2,390	0.611		12,800	1.966
3	2,580	0.653	6	13,000	1.970
	2,769	0.675		13,200	1.985
	2,958	0.696		13,400	2.000
	3,147	0.723		13,600	2.020
	3,336	0.746		13,800	2.030
	3,525	0.768		14,000	2.055
	3,714			14,200	
	3,903	0.816		14,400	2.095
	4,092	0.838		14,600	2.115
	4,281	0.856		14,800	2.125
	4,470	0.888		15,000	2.137
	4,659	0.905		15,200	2.150

* Distance from Shot Point 2 at northwest end of line

Line B continued

Spread	Distance*	Time	Spread	Distance**	Time
7	15,400	2.136	1	1,300 NW	0.419
	15,600	2.186		1,200	0.399
	15,800	2.205		1,100	0.398
	16,000	2.245		1,000	0.388
	16,200			900	0.369
	16,400			800	
	16,600			700	0.334
	16,800	2.285		600	0.322
	17,000	2.309		500	0.300
	17,200	2.304		400	0.258
	17,400	2.315		300	0.209
	17,600	2.315		200	0.160
			2	200 SE	0.157
				300	0.208
				400	0.264
				500	0.304
				600	0.309
				700	0.318
				800	
				900	0.343
				1,000	0.345
				1,100	0.352
				1,200	0.365
				1,300	0.371
			3	1,300	0.370
				1,500	0.393
				1,700	0.418
				1,900	0.441
				2,100	0.458
				2,300	0.495
				2,500	0.524
				2,700	0.555
				2,900	0.584
				3,100	0.618
				3,300	0.645
				3,500	0.674

Distance between Shot Points 2 and 3: approximately 11,900'

* Distance from Shot Point 2

** Distance from Shot Point 3

Line B continued

Spread	Distance*	Time
1	205	0.092
	405	0.135
	605	0.162
	805	0.188
	1,005	0.218
	1,205	0.244
	1,405	0.275
	1,605	0.292
	1,805	0.318
	2,005	0.340
	2,205	0.378
	2,405	0.402
2	2,608	0.414
	2,808	0.446
	3,008	0.471
	3,208	0.496
	3,408	0.526
	3,608	0.553
	3,808	0.576
	4,008	0.606
	4,208	0.626
	4,408	0.647
	4,608	0.662
	4,808	0.685
3	6,008	0.808
	6,208	0.826
	6,408	0.842
	6,608	0.863
	6,808	0.888
	7,008	
	7,208	0.924
	7,408	0.948
	7,608	0.968
	7,808	0.990
	8,008	1.013
	8,208	1.038
	8,408	1.051
	8,608	1.083
	8,808	1.105
	9,008	1.129

Distance between Shot Points 2 and 4: approximately 21,208'

* Distance from Shot Point 4 at southeast end of line

SEISMIC DATA - LINE C

Spread	Distance*	Time
1	300	0.205
	500	0.298
	700	0.362
	900	0.402
	1,100	0.435
	1,300	0.471
	1,500	
	1,700	0.529
	1,900	0.563
	2,100	0.593
	2,300	0.628
	2,500	0.663
2	2,715	0.708
	2,915	0.763
	3,115	0.766
	3,315	0.798
	3,515	0.830
	3,715	0.861
	3,915	
	4,115	0.921
	4,300	0.945
	4,500	0.962
	4,700	0.996
	4,900	1.027
3	5,750	1.172
	5,945	1.201
	6,140	1.224
	6,335	1.253
	6,530	1.284
	6,725	
	6,920	1.330
	7,065	1.360
	7,260	1.382
	7,445	1.404
	7,640	1.441
	7,835	1.461

* Distance from Shot Point 2 at northeast end of line

Line C continued

Spread	Distance*	Time	Distance#	Time	Spread
4	8,035	1.500	3,377	0.539	2
	8,235	1.520	3,178	0.513	
	8,435	1.545	2,979	0.498	
	8,635	1.575	2,780	0.468	
	8,835	1.600	2,581	0.449	
	9,035	1.610	2,382	0.428	
	9,235		2,185		
	9,435	1.611	1,990	0.376	
	9,615	1.613	1,793	0.355	
	9.795	1.613	1,605	0.332	
	9,975	1.600	1,425	0.308	
	10,155	1.607	1,250	0.291	
			1,100	0.265	1
			1,000	0.249	
			900	0.230	
			800	0.213	
			700	0.204	
			600	0.191	
			500		
			400	0.137	
			300	0.117	
			200	0.079	
			100	0.038	
			25	0.015	
1**	51***	0.050	800##	0.359	1###
	151	0.137	900	0.358	
	251	0.191	1,000	0.364	
	351	0.232	1,100	0.372	
	451	0.279	1,200	0.374	
	551		1,300		
	651	0.298	1,400	0.374	
	751	0.286	1,500	0.374	
	851	0.283	1,600	0.349	
	951	0.277	1,700	0.354	
	1,051	0.270	1,800	0.349	
	1,151	0.276	1,900	0.349	

* Distance from Shot Point 2 at northeast end of line

# Distance from Shot Point 5 at southwest end of line

** Same recording location as Spread 1 for Shot Point 5

*** Shot Point 5a 51 feet northeast of spread

## Shot Point 5b 800 feet northeast of spread

### Same recording location as Spread 1 for Shot Point 5

SEISMIC DATA - LINE D

Spread	Distance*	Time	Spread	Distance**	Time
1	1,300 NE	0.380	1	1,300 SW	0.242
	1,200	0.361		1,200	0.240
	1,100	0.350		1,100	0.234
	1,000	0.340		1,000	0.233
	900	0.329		900	0.229
	800			800	0.232
	700	0.322		700	0.231
	600	0.309		600	0.226
	500	0.294		500	0.213
	400	0.243		400	0.208
	300	0.198		300	0.170
	200	0.149		200	0.125
2	420 SW	0.266	2	200 NE	0.111
	520	0.297		300	0.164
	620	0.326		400	0.215
	720	0.359		490	0.250
	820	0.380		590	0.263
	920			689	0.269
	1,020	0.409		788	0.270
	1,120	0.420		885	0.294
	1,220	0.438		980	0.314
	1,320	0.454		1,078	0.320
	1,420	0.464		1,175	0.328
	1,520	0.465		1,270	0.338
3	1,520	0.477	3	1,280	0.334
	1,720	0.487		1,477	0.353
	1,920	0.500		1,674	0.374
	2,120	0.520		1,871	0.384
	2,320	0.544		2,068	0.405
	2,520	0.570		2,265	0.419
	2,720	0.584		2,462	0.449
	2,920	0.603		2,659	0.468
	3,120	0.613		2,856	0.489
	3,320	0.636		3,056	0.506
	3,520	0.660		3,256	0.521
	3,720	0.676		3,456	0.540

Distance between Shot Points 3 and 6a: 5,000 feet

* Distance from Shot Point 3

** Distance from Shot Point 6a

Line D continued

Spread	Distance*	Time
1	3,380	0.412
	3,577	0.435
	3,774	0.452
	3,971	0.461
	4,168	0.485
	4,365	0.505
	4,562	0.525
	4,759	0.541
	4,956	0.561
	5,156	0.580
	5,356	0.591
	5,556	0.608

Distance between Shot Points 6 and 6a: 2,100 feet

Distance between Shot Points 3 and 6: 7,100 feet

* Distance from Shot Point 6 at southwest end of line

PUBLISHED GEOLOGICAL INFORMATION RELEVANT TO THE SAN JACINTO GROUND WATER BASIN

A brief abstract or comments follow some of the references. The references are presented in chronological order.

1857 Blake, W. P., Geological report (Williamson's reconnaissance in California) U. S. Pacific railroad exploration; U. S. 33rd Cong., 2d sess., S. Ex. Doc. 78 and H. Ex. Doc. 91, vol. 5, pt. 2, 370 p.

Map 4, covering most of southern California, is at a scale of 1:1,500,000.

1871 Guillemin-Tarayre, E., Description des anciennes possessions mexicaines du nord: Mission Scientifique au Mexique et dans l' Amerique Centrale, Geologie pt. 2, 216 p.

Plate 15 covers southern California west of approximately 116° 50' west longitude at a scale of 1:1,000,000.

1886 Hanks, H. G., San Diego County: California Min. Bur. 6th Ann. Rept. pt. 1, pp. 80-90.

The map covers the southeastern half of the San Jacinto ground water basin at a scale of 1:375,000.

1893 Fairbanks, H. W., Geology of San Diego County; also portions of Orange and San Bernardino Counties: California Min. Bur. 11th Ann. Rept., pp. 76-120.

The map covers almost all of the San Jacinto ground water basin at a scale of 1:375,000.

1899 The Riverside PRESS AND HORTICULTURIST, December 30th.

A newspaper article describes the San Jacinto earthquake of December 25, 1899. The south walls of brick buildings "invariably went down, most of them falling outward."

1900 Claypole, E. W., The earthquake of San Jacinto, December 25, 1899; Am. Geologist, vol. 25, pp. 106-108.

In Hemet, almost all brick buildings were severely damaged and only two chimneys remained standing. Six people were killed and eight injured at Soboba. Ten miles southeast of San Jacinto there were many fresh surface cracks and it is possible that the earthquake centered near here. Some damage was done to Riverside and the shock was distinctly felt at San Diego and at Seligman, Arizona. Aftershocks occured through May of 1900.

1907 Danes, J. V., Das Erdbeben von San Jacinto am 25 December 1899; Mitteilungen der K. K. Geogr. Gesellschaft in Wien, Heft 6-7, pp. 339-347.

A report of the San Jacinto earthquake of December 25, 1899.

1908 Lawson, A. C., and others. The California earthquake of April 18, 1906; Carnegie Inst. Wash. Pub. 87, vol. 1, 451 p.

This report of an earthquake investigation committee includes a reconnaissance of the San Andreas fault system. It shows the San Jacinto fault as a continuous break from the San Jacinto Valley to the Borrego Valley.

1908 Hess, F. L., The Magnesite deposits of California;

U. S. Geological Survey Bull. 355, 67 p.

The bulletin contains a brief description of the serpentine in the vicinity of the magnesite mine south of Hemet airport.

1912 Gale, Hoyt S., Late developments of magnesite deposits in California and Nevada; U. S. Geological Survey Bull. 540, pp. 483-520.

Gale's article contains more information on the magnesite mine south of Hemet airport. Figure 54 is a geological map at a scale of 1:13,500.

1915 Beal, Carl H., The earthquake in the Imperial Valley, California, June 22, 1915; Bulletin of the Seismological Soc. of Am., vol. 5, pp. 130-149.

Beal maps the San Jacinto fault as a single fault line passing north of the town of San Jacinto, apparently at the southwest base of the mountains north of San Jacinto.

1918 Townley, Sidney D., The San Jacinto earthquake of April 21, 1918; Bulletin of the Seismological Soc. of Am., vol. 8, pp. 44-62.

The article contains several pictures of the damage caused by this earthquake - and there was much damage. The quake was felt over all of southern California and western Arizona. Fortunately the quake occured on a Sunday afternoon so few people were in the business districts. Many injuries resulted but no deaths. The concrete road between Hemet and San Jacinto was cracked in thirteen places and the concrete road running northwesterly from San Jacinto was seriously cracked and buckled. Many live limbs were shaken from trees. A number of landslides occured in the San Jacinto mountains, one swept a car off the road. The ground was cracked in several places throughout the valley as were irrigation canals.

1918 Rolfe, Frank and A. M. Strong, The earthquake of April 21, 1918, in the San Jacinto Mountains; Bulletin of the Seismological Soc. of Am., vol. 8, pp. 63-67.

A description of the earthquake effects on the area to the south and east of San Jacinto Valley is given.

1918 Arnold, Ralph, Topography and fault system of the region of the San Jacinto earthquake; Bulletin of the Seismological So. of Am., vol. 8, pp. 68-73.

The main branch of the San Jacinto fault zone is located as passing through Hog Lake, the Blackburn ranch, by the northeastern side of Park Hill and under the town of San Jacinto.

1918 The Los Angeles TIMES, April 23, 1918.

A newspaper article describes the San Jacinto earthquake of April 21, 1918. "There were nine separate temblors over a period of thirty hours, beginning Sunday at 3:32 o'clock p. m."

1919 Waring, G. A., Ground water in the San Jacinto and Temecula basins, California; U.S. Geological Survey Water Supply Paper 429.

Waring's water supply paper represents a detailed starting point of recorded information on the ground water of these two basins. It describes water use, quality, level, origin and fluctuation. The likelihood of overdraft is pointed out and many well logs are presented.

1920 Hill, R. T., The rifts of Southern California; Bulletin of the Seismological Soc. of Am., vol. 10, pp. 146-149.

Little new information is presented. Hill expresses his feeling that too much concern is given to the destructive effects of earthquakes.

1921 Frick, Childs, Extinct vertebrate faunus of the Badlands of Bautista Creek and San Timoteo Canyon, southern California; Univ. Calif. Pub., Bull. Dept. Geol. Sci., vol. 12, no. 5, pp. 277-424.

A paleontological dating of the sediments of the badlands on the edges of the San Jacinto ground water basin is presented.

1924 Woodford, A. O., The Catalina metamorphic facies of the Franciscan series; Calif. Univ. Dept. Geol. Sci. Bull., vol. 15, no. 3, pp. 49-68.

Figure 1 of Woodford's article is a geological map at a scale of 1:1,500,000 that includes portions of San Diego, Orange, and Riverside counties. The northeastern corner of this map includes Winchester, Romoland, Homeland, and the Menifee areas. Since the publication of this article, more detailed mapping of these areas has been published.

1926 English, W. A., Geology and oil resources of the Puente Hills region, southern California; U.S. Geological Survey Bull. 768, 110 p.

In this bulletin English names the rather stable geologic area between the San Jacinto and the Elsinore fault zones the "Perris fault block." This is about the only item in the bulletin that is pertinent to the San Jacinto basin.

1928 Hill, R. T., Southern California geology and Los Angeles earthquakes; Published by Southern Calif. Acad. Sci., Los Angeles, 232 p.

Hill states that from 1780 to 1928 there were 170 reported shocks in southern California; 92 on the San Jacinto rift, 16 on the San Andreas rift, 16 on the Elsinore rift, 14 near Inglewood, 2 near Los Angeles city and 30 shocks from distant localities.

1928 Post, W. S., Santa Ana investigation, flood control and conservation; California Div. Engr. and Irrigation Bull. 19, 367 p.

Map 14, at a scale of 1:250,000, includes most of the San Jacinto ground water basin.

1931 Fraser, D. M., Geology of San Jacinto quadrangle south of San Gorgonio Pass, California; Mining in Calif. (Calif. Jour. of Mining and Geology,) vol. 27, pp. 494-540.

Though somewhat reconnaissant in coverage, this article, a condensation of Fraser's doctoral dissertation contains many observations of interest to any geological study in the area. His map is at a scale of 1:125,000 and extends as far west as 117° west longitude, approximately Sanderson street.

1932 Sampson, R. J., Economic mineral deposits of the San Jacinto quadrangle; Mining in Calif. (Calif. Jour. of Mining and Geology,) vol. 28, pp. 3-11.

The map scale is 1:125,000 and is of no interest to ground water studies.

1933 Murdoch, Joseph, Andalusite in pegmatite; Am. Mineralogist, vol. 21, pp. 68-69.

Murdoch gives a discription of the pegmatites associated with the serpentines of the magnesite mine area south of Hemet airport.

1934 Eckis, R., South Coastal Basin investigation; Geology and ground water storage capacity of valley fill; Calif. Div. Water Resources Bull. 45, 279 p.

Though this bulletin does not cover the San Jacinto ground water basin, Bean's estimate of the specific yield in the San Jacinto - Hemet area (Bean, 1955) is based on results of this bulletin.

1935 Sampson, R. J., Mineral resources of a portion of the Perris Block, Riverside county, Calif.; Calif. Jour. of Mines and Geology, vol. 31, pp. 507-521.

Though historically interesting, Sampson's article is of no interest to ground water studies

1935 Dudley, P. H., Geology of a portion of the Perris Block, southern California; Calif. Jour. of Mines and Geology, vol. 31, pp. 487-506.

The major emphasis of Dudley's article is the igneous and metamorphic rocks, their petrology and the sequence of their emplacement.

1936 Dudley, P. H., Physiographic history of a portion of the Perris Block, southern California; Jour. Geol., vol. 44, pp. 358-378.

In order to understand the more recent geological history of the Perris Block, this article examines the erosional and fault land forms. It is an assistance in understanding the bedrock features below the valley sediments.

1937 Axelrod, D. I., A Pliocene flora from the Mt. Eden beds, southern California; Carnegie Inst. Washington, Pub. 476, pp. 125-184.

The badland sediments north of the San Jacinto valley are dated with the aid of plant fossils.

1939 Henderson, L. H., Detailed geological mapping and fault studies of the San Jacinto tunnel line and vicinity; Jour. Geol., vol. 47, pp. 314-324.

Over twenty faults, parallel or subparallel to the San Jacinto fault zone, are mapped and their effect on

the San Jacinto tunnel is reported. These faults produced much water and caused severe problems during the driving of the tunnel.

1939 Osborn, E. F., Structural petrology of the Val Verde tonalite, southern California; Geol. Soc. America Bull., vol. 50, pp. 921-950.

The basement rock west of a portion of the Perris sub-basin of the San Jacinto ground water basin is examined in this article.

1939 Webb, Robert W., Evidence of the age of a crystalline limestone in southern California; Jour. Geol., vol. 47, pp. 198-201.

Webb found Carboniferous (Mississippian) fossils in the limestone interbedded with the schists north and south of Domenigoni valley and thus helped date the older metamorphic rocks around and below part of the San Jacinto basin.

1948 Larsen, E. S., Jr., Batholith and associated rocks of Corona, Elsinore, and San Luis Rey quadrangles, southern California; Geol. Soc. America Mem. 29, 182 p.

Most of the information of Larsen's memoir is contained in his 1951 Calif. Div. of Mines bulletin.

1949 Sprotte, E. C., The San Andreas and San Jacinto fault zones; Sigma Gamma Epsilon, The Compass, vol. 26, pp. 315-319.

1950 Axelrod, D. I. Further studies of the Mt. Eden flora, southern California; Carnegie Inst. Washington, Pub. 590, pp. 73-118.

1951 Larsen, E. S., Jr., Crystalline rocks of the Corona, Elsinore, and San Luis Rey Quadrangles, southern California; Calif. Div. of Mines bulletin 159, pp. 7-50.

The petrology and relative age of the basement rocks are discussed in detail but little information is presented about the faults and almost no information about the water bearing sediments. Larsen's map is at a scale of 1:125,000 and indicates the type of exposed crystalline rocks in and around the portion of the San Jacinto ground water basin that is west of 117° west longitude (approximately Sanderson street.) Larsen's work can be of assistance in obtaining estimates of the relative permiabilities of the crystalline rocks.

1954 Jahns, R. H., Geology of the Peninsular range province, southern California and Baja California; Calif. Div. of Mines Bull. 170, chapter II, pp. 29-52.

The San Jacinto ground water basin is in the northern part of the Peninsular range. Jahns' article gives a clear understanding of the geological framework of which the San Jacinto basin is a small part.

1954 Jahns, R. H., Northern part of the Peninsular range province; Calif. Div. of Mines Bull. 170, geologic guide No. 5, 59 p.

This guide book presents a tour of the geology sur-

rounding, but not including, the San Jacinto ground water basin. It is accompanied by several geologic maps.

1954 Gray, Cliffton H., Geology of the Corona-Elsinore-Murrieta area, Riverside county; map sheet No. 21, Calif. Div. of Mines Bull. 170.

This includes the southwestern portion of the San Jacinto ground water basin. This portion of the map is based on Dudley (1935 and 1936) and Larsen (1948) and little or no new information is presented.

1955 Kundert, C. J., Santa Ana Sheet; Geological Map of California, Calif. Div. of Mines.

In the area of the San Jacinto ground water basin this map is based on Larsen (1951) and Fraser (1931) and no new information is presented. The scale is 1:250,000. The map has been reissued in 1965 and contains more detailed information. See 1965, Rogers.

1955 Bean, Robert T., Geology of San Jacinto and Elsinore basins, appendix B, Santa Ana river investigation; bulletin No. 15, Calif. State Water Resources Board, 88 p.

Bean's report covers in detail the ground water geology and geology of the water bearing sediments. The areal geology of the crystalline rocks is based on previous work by other geologists.

1959 Engel, Rene, Geology and mineral deposits of the Lake Elsinore quadrangle, California; Calif. Div. of Mines Bull. 146, 154 p.

Bulletin 146 just touches the southwestern corner of the San Jacinto ground water basin near Railroad canyon reservoir. In that area the igneous and metamorphic rocks are maped in somewhat more detail than by Larsen (1951.) Engel's Santa Ana formation is called Bedford Canyon formation by Larsen and most other geologists. The map scale is 1:62,500.

1962 Proctor, R. J., Geologic features of a section across the Casa Loma fault, exposed in an aqueduct trench near San Jacinto, California; Geological Soc. Am. Bull., vol. 73, pp. 1293-1296.

Evidence of very recent movement of the Casa Loma fault is reported.

1964 Eaton, G. N., Martin, and M.A. Murphy, Application of gravity measurements to some problems in engineering geology; Engineering Geology, vol. 1, no. 2, pp. 6-21.

Northeast of Perris a gravity survey was performed. Knowing the depth to basement rock from test hole information and knowing the density of basement rock and the grain density of the sediments, it was possible to estimate the porosity of the sediments. A porosity of 36 to 40 percent was indicated.

1965 Rogers, Thomas H., Santa Ana Sheet; Geologic Map of California, Calif. Div. of Mines.

Rogers compiled this geologic map and did some of the mapping. The San Jacinto basin portion of the map is based primarily on Bean's 1955 work.

1967 Fett, J.D., D.H. Hamilton, and F.A. Fleming, Continuing surface displacements along the Casa Loma and San Jacinto faults in San Jacinto Valley, Riverside County, California; Engineering Geology, vol. 4, no. 1, pp 22-32

Displacement and pipeline and road fracturing along these faults are reported. The city of San Jacinto subsided more than a foot in the period 1932-1964. More recent work establishes the cause of current subsidence to be ground water withdrawal (Fett and Hamilton, in preparation and to be submitted to Engineering Geology.)

1967 Sharp, Robert V., San Jacinto fault zone in the Peninsular Ranges of Southern California; Bull. Geol. Soc. Am., vol. 78, no. 6, pp 705-730.

This paper is based on Sharp's doctoral dissertation. The San Jacinto fault zone and adjacent geology have been investigated from the southeast end of San Jacinto valley to the Borrego Valley area. Fifteen miles of right-lateral displacement has occured as well as one to two miles of vertical displacement, the northeast side dropping with relation to the southwest side.

1 Accession Number W 70-05466	2 Subject Field & Group 05D 04B, 05E, ~~02F~~	**SELECTED WATER RESOURCES ABSTRACTS** **INPUT TRANSACTION FORM**

5 Organization
Eastern Municipal Water District, Hemet, California.

6 Title
REUTILIZATION OF WASTEWATER RECYCLED THROUGH GROUND WATER, VOLUME 1 AND 2,

10 Author(s)

16 Project Designation
Grant FWPCA 16060 DDZ --- 12/67

21 Note
~~Report available for inspection in USGS-WRD~~
Library, ~~Wash, D C.~~
Available from the Clearing-
house as PB 190790 (Vol. I), and PB 190791 (Vol. II)
$3 in paper copy, 65¢ in microfiche

22 Citation
Progress Report to Federal Water Pollution Control Administration for Project 16060, December 1968. Volume 1 - 125 p, 45 fig, 20 tab, 13 ref. Volume 2 - 87 p, 61 ref, 3 append.

23 Descriptors (Starred First)
*Artificial recharge, *Water reuse, *California, Water yield, Infiltration, Water spreading, Pit recharge, Safe yield, Water balance, Hydrogeology, Data collections, Hydrologic data, Groundwater movement, Water quality, Water levels, Water supply, Water utilization, Surveys, Geophysics.

25 Identifiers (Starred First)
San Jacinto Valley (Calif).

27 Abstract
The water quality factors involved in the recharging of the San Jacinto Basin, California are evaluated so that the overall operation may be conducted in a manner to provide adequate protection of groundwater quality while permitting reclamation of wastes for regional water conservation. Another objective is to study the benefits to the salt balance problem caused by recharging. In the previous situation, some effluents were discharged to the San Jacinto River area and some were used as irrigation water. With recharge there is a significant reduction in evapotranspiration losses, thus improving groundwater quality by diluting the dissolved salts. The safe groundwater yield is limited to approximately 11,205 acre-feet/year. The volumes of water reclaimed and put underground to replenish the overdraft now average approximately 1430 acre-feet/year. Withdrawals now approximate 12,000 acre-feet/year, and importation of Colorado River water approximates 1900 acre-feet/year. Inflow of salt into the basin is now estimated at 5800 ton/year; 3900 ton/year from inflowing groundwater and 1900 ton/year from imported Colorado River water. (Knapp-USGS)

Abstractor George Knapp 3-24-70	Institution U. S. Geological Survey, Water Resources Div.

WR 102 (REV. JULY 1969)
WRSIC

SEND TO: WATER RESOURCES SCIENTIFIC INFORMATION CENTER
U.S. DEPARTMENT OF THE INTERIOR
WASHINGTON, D. C. 20240